Large-Scale Changes of Soil Wetness Induced by an Increase in Atmospheric Carbon Dioxide

S. MANABE AND R. T. WETHERALD

Geophysical Fluid Dynamics Laboratory/NOAA, Princeton University, Princeton, NJ 08542

(Manuscript received 29 May 1986, in final form 17 November 1986)

ABSTRACT

The change in soil wetness in response to an increase of atmospheric concentration of carbon dioxide is investigated by two versions of a climate model which consists of a general circulation model of the atmosphere and a static mixed layer ocean. In the first version of the model, the distribution of cloud cover is specified whereas it is computed in the second version incorporating the interaction among cloud cover, radiative transfer and the atmospheric circulation. The CO_2-induced changes of climate and hydrology are evaluated based upon a comparison between two quasi-equilibrium climates of a model with a normal and an above normal concentration of atmospheric carbon dioxide.

It is shown that, in response to a doubling (or quadrupling) of atmospheric carbon dioxide, soil moisture is reduced in summer over extensive midcontinental regions of both North America and Eurasia in middle and high latitudes. Based upon the budget analysis of heat and water, the physical mechanisms responsible for the CO_2-induced changes of soil moisture are determined for the following four regions: northern Canada, northern Siberia, the Great Plains of North America and southern Europe. It is found that, over northern Canada and northern Siberia, the CO_2-induced reduction of soil moisture in summer results from the earlier occurrence of the snowmelt season followed by a period of intense evaporation. Over the Great Plains of North America, the earlier termination of the snowmelt season also contributes to the reduction of soil moisture during the summer season. In addition, the rainy period of late spring ends earlier, thus enhancing the CO_2-induced reduction of soil moisture in summer. In the model with variable cloud cover, the summer dryness over the Great Plains is enhanced further by a reduction of cloud amount and precipitation in the lower model atmosphere. This reduction of cloud amount increases the solar energy reaching the continental surface and the rate of potential evaporation. Both the decrease of precipitation and the increase of potential evaporation further reduce the soil moisture during early summer and help to maintain it at a low level throughout the summer. Over Southern Europe, the CO_2-induced reduction of soil wetness occurs in a qualitatively similar manner, although the relative magnitude of the contribution from the change in snowmelt is smaller.

During winter, soil moisture increases poleward of 30°N in response to an increase of atmospheric carbon dioxide. Because of the CO_2-induced warming, a greater fraction of the total precipitation occurs as rainfall rather than snowfall. The warmer atmosphere also causes the accumulated snow cover to melt during winter. Both processes act to increase the soil moisture in all four regions during the winter season. The increase of soil moisture is enhanced further in high latitudes due to the increase of precipitation resulting from the penetration of warm, moisture-rich air into higher latitudes.

The CO_2-induced warming of the lower model troposphere increases with increasing latitude. The present analysis suggests that the changes of soil wetness described in this investigation are controlled by the latitudinal profile of the warming and are very broad scale, mid-continental phenomena.

1. Introduction

This study investigates the effect of an increase of the atmospheric concentration of carbon dioxide on soil wetness. It represents a continuation of the earlier study by Manabe et al. (1981) which explored a similar topic. Performing numerical experiments with a general circulation model of the atmosphere coupled with a static mixed layer model of oceans, they tried to identify the CO_2-induced change in the hydrology of the continental surface. The results from these experiments indicated a significant CO_2-induced reduction in the zonal mean wetness of the continental surface in middle and high latitudes during summer. Because of the limited availability of computer time, the period of the numerical time integration of their model was not long enough to extract reliably the geographical distribution of the CO_2-induced change from the natural variation of soil moisture. Therefore, their study was mainly concerned with the zonally averaged rather than the geographical distribution of the CO_2-induced change of soil wetness.

Since the publication of the study by Manabe et al., the results from several later studies of the CO_2-induced changes of climate have become available. For example, Mitchell and Lupton (1984) used a general circulation model with a relatively high computational resolution and prescribed sea surface temperature for the study of this problem. In their control integration, sea surface temperature was prescribed from climatol-

ogy. However, in the doubled CO_2-experiment, the changes in sea surface temperature are prescribed such that the ocean, as a whole, is in approximate thermal equilibrium with the atmosphere. In qualitative agreement with the result of Manabe et al., their experiment indicates the summer reduction of soil moisture over extensive midcontinental regions of both the North American and Eurasian continents.

CO_2-climate sensitivity studies were also conducted by Hansen et al. (1984) and Washington and Meehl (1984). Both studies used an atmosphere mixed layer model, though the distribution of cloud cover was predicted rather than prescribed. According to the review paper by Schlesinger and Mitchell (1985), the zonal mean soil moisture in the model of Hansen et al. was reduced slightly in middle latitudes of the Northern Hemisphere in response to the doubling of atmospheric carbon dioxide. However, the magnitude of the reduction is much less than that obtained in the study of Manabe et al. In the experiment conducted by Washington and Meehl, zonal mean soil moisture increased slightly in summer responding to a doubling of atmospheric carbon dioxide even though some continental regions showed decreases (e.g., central North America and western Europe).

Although the CO_2-induced change of zonal mean soil moisture over the continents of the Northern Hemisphere is positive during winter in all three experiments, the corresponding change during summer differs qualitatively from one experiment to another as described above. Unfortunately, a detailed analysis of the seasonal variation of the surface water budget in these experiments is not available at the present time. Therefore, a critical intercomparison among these results must await the publication of such an analysis.

With regard to the geographical distribution of the CO_2-induced soil moisture change, it has been particularly difficult to establish a coherent pattern from the results of the studies previously mentioned. (See, for example, the intercomparison of the results from these studies conducted by Schlesinger and Mitchell, 1985.)

This study attempts to determine the very broad-scale features of the geographical distribution of the soil wetness and its seasonal variation based upon the results from several numerical experiments conducted at the Geophysical Fluid Dynamics Laboratory of NOAA. The lengths of the numerical time-integrations in these experiments are chosen to be much longer than those in the study of Manabe et al. in order to insure that the period of stable equilibrium towards the end of each integration is long enough to detect the CO_2-induced change from the natural variability of the model hydrology. When broad-scale, CO_2-induced changes of soil wetness are found to be statistically significant and common among the results of several experiments conducted here, the physical mechanisms responsible for these changes are investigated based upon a detailed analysis of the surface water budget. In contrast to the study of Manabe et al. in which only a zonally averaged water budget was evaluated, this analysis was performed over several very large domains in the Eurasian and North American continents. It is hoped that the results from the present analysis will provide a basis for a comparative assessment of the various studies in the future.

In the study of Manabe et al., (1981) it is assumed that the distribution of cloud cover is unchanged despite the increase in the CO_2-concentration of the atmosphere. However, it is very likely that the CO_2-induced change in soil wetness modifies the rate of evaporation, and accordingly, alters the rate of precipitation and cloud coverage thereby influencing the budget of heat and water over the continental surfaces. Therefore, the numerical experiments in the present study are conducted by the use of two versions of a model with and without the cloud feedback process. (Hereafter, these two versions of the model are called "variable cloud (VC) model" and "fixed cloud (FC) model," respectively.) By comparing the results from these two versions of the model, the influence of the cloud-radiation feedback process upon the CO_2-induced change in soil wetness is evaluated.

The fixed cloud model used in the present study is very similar to the model of Manabe et al., although the albedoes of snow cover and sea ice are slightly modified and a different distribution of cloud is prescribed as explained in section 2. In both fixed and variable cloud models, the oceanic component of this model is a static mixed layer without ocean currents. It is expected that the absence of oceanic heat transport in the model significantly affects the distribution of sea surface temperature and its CO_2-induced changes. Thus, this study should be regarded as a prelude to the more definitive, future study in which the effects of ocean currents are taken into consideration.

(A brief summary of the results from the present study was recently published: Manabe and Wetherald, 1986.)

2. Atmosphere-mixed layer ocean model

a. Structure

The mathematical model of climate used for this research is an atmospheric general circulation model coupled with a static mixed layer ocean model. The atmospheric portion of the model predicts the changes of the vertical components of vorticity and divergence, temperature, surface pressure and moisture based upon the equations of motion, the thermodynamical equation, and the continuity equations of mass and moisture. The horizontal distributions of these variables are represented by a limited number of spherical harmonics (i.e., the first 15 modes in both zonal and meridional directions). The vertical distributions are specified at nine unequally spaced finite difference levels. The dynamical component of the model just described is de-

veloped by Gordon and Stern (1982). The model has a global computational domain, realistic geography as well as land–sea contrast and seasonally varying insolation.

For the computation of solar and terrestrial radiation, the distribution of ozone is prescribed and the concentration of carbon dioxide is assumed to be constant everywhere. The distribution of water vapor is determined from the prognostic equation of water vapor. The fields of both solar and terrestrial radiation are also affected by the presence of cloud cover. As explained in the Introduction, two versions of the model are constructed. In the first version, i.e., the FC model, the latitudinal distributions of total cloud cover is taken from Berlyand et al. (1980) and the vertical distribution from London (1957). In the second version, i.e., the VC-model, cloud cover is predicted wherever the relative humidity exceeds 99%. (This critical value of relative humidity is chosen such that the globally averaged total cloud amount is about 55%.) The two versions are identical in all other respects.

Precipitation is computed whenever supersaturation is indicated by the prognostic equation for water vapor. It is identified as snowfall when the air temperature near the surface falls below freezing; otherwise it is identified as rain. The moist convective processes are parameterized by a moist convective adjustment scheme as proposed by Manabe et al. (1965).

The temperature of the continental surface satisfies the condition of local thermal balance among the various components of the surface heat budget. A change in snow depth is computed as a net contribution from snowfall, sublimation and the snowmelt which is determined from the requirement of surface heat balance (see Manabe, 1969 for further details). The soil albedo is prescribed geographically by referring to the study of Posey and Clapp (1964) but is replaced by a temperature dependent higher value over snow covered regions.

The budget of soil moisture is computed by the so-called bucket method. Within the model, soil is assumed to have the ability to contain 15 cm of liquid water. (This is known as the "field capacity".) When the soil is not saturated with water, the change of soil moisture is predicted as a net contribution of rainfall, evaporation and snowmelt. If the soil moisture value reaches the field capacity (i.e., the bucket is full), the excess water is regarded as runoff. The rate of evaporation from the soil surface is determined as a function of the water content of the "bucket" and potential evaporation, i.e., hypothetical evaporation rate from a completely wet surface (for further details of soil moisture prediction, see Manabe, 1969).

The oceanic portion of the model is a static isothermal layer of sea water with a uniform thickness of 50 meters. The ocean temperature change is computed from the budget of surface heat fluxes. The effects of horizontal heat transport by ocean currents and heat exchange between the mixed layer and the deeper layer of the ocean are neglected. The changes in sea ice thickness are computed from the processes of melting of ice and freezing of sea water, sublimation and snowfall as proposed by Bryan (1969). The ocean albedo is prescribed as a function of latitude but is replaced by a higher value over oceanic regions covered by sea ice.

The FC-model used here is very similar to the model developed by Manabe and Stouffer (1980) with the exception of the treatment of cloud cover. As mentioned earlier, the distribution of cloud cover differs from one hemisphere to another in the present model, whereas it is essentially symmetric in their model. This difference in the distribution of cloud cover is responsible for the more realistic simulation of surface air temperature in the Southern Hemisphere of the present FC model. See Manabe and Broccoli, (1985) for further discussion of this topic.

b. Performance

The geographical distributions of precipitation rate from both FC- and VC-models resemble the distribution obtained from the model constructed by Manabe and Stouffer (1980). (See Figs. 10a, b of their paper.) Therefore, these distributions are not shown here. To provide a glimpse of the model performance in simulating the hydrology of continental surface, the global distributions of annual mean rate of runoff from both FC- and VC-models are compared (in Fig. 1) with the corresponding distribution of the actual runoff estimated by Lvovitch and Ovtchinnikov (1964). According to this figure, the distributions of runoff from the two models resemble each other. It is encouraging that both models reproduce the major arid regions with small runoff in the Sahara and central Asian regions of the Northern Hemisphere and in Australia, Kalahari and Patagonia of the Southern Hemisphere. They also simulate the areas of large runoff in the northwestern region of North America and Southeast Asia. On the other hand, one can identify various unrealistic features in the simulated distribution. For example, the rate of runoff in the southwestern part of North America is not small enough and the area of meager runoff in the Gobi and Sahara deserts is too narrow. Also the model underestimates the runoff over Northern Brazil. Nevertheless, the comparison in Fig. 1 reveals that the models successfully reproduce very gross characteristics of the global distribution of the observed runoff.

Another indicator of the model's performance is illustrated by Fig. 2 which shows the geographical distributions of soil moisture from the FC-model for the periods of June–July–August and December–January–February. An examination of the June–August distribution reveals that, again, soil moisture is low in the major arid regions such as the Sahara and Gobi deserts as well as the southwestern United States. Also evident are the relatively wet continental areas in the vicinity

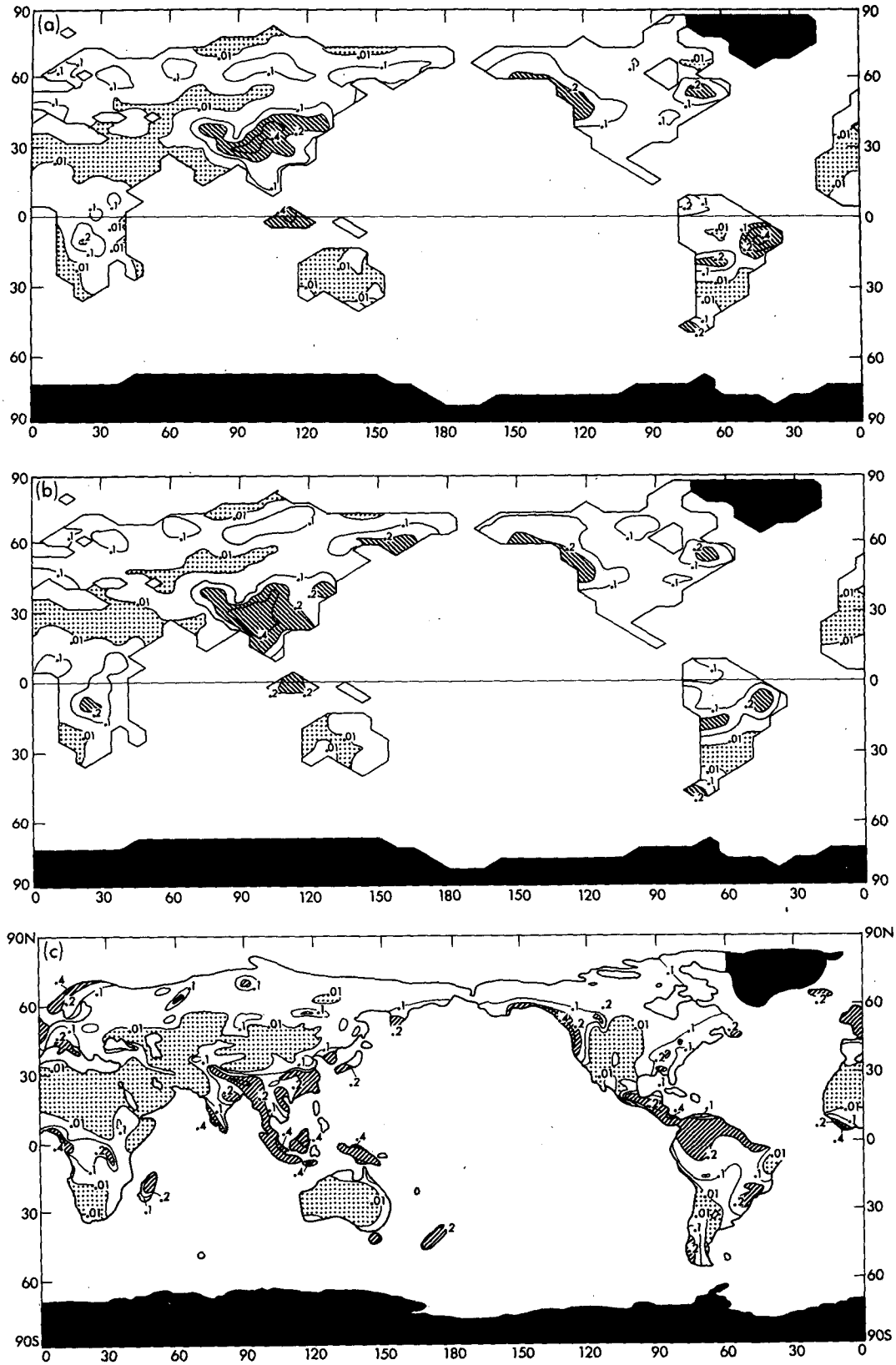

FIG. 1. Global distribution of annual mean rate of runoff (cm day^{-1}). (a) FC-model, (b) VC-model, (c) observed distribution compiled by Lvovitch and Ovchinnikov (1964). Note that some artificial smoothing is made in the process of copying the map of observed distribution. The slanted and shaded areas indicate the regions where the rate of runoff is more than 0.2 cm day^{-1} and less than 0.01 cm day^{-1}, respectively.

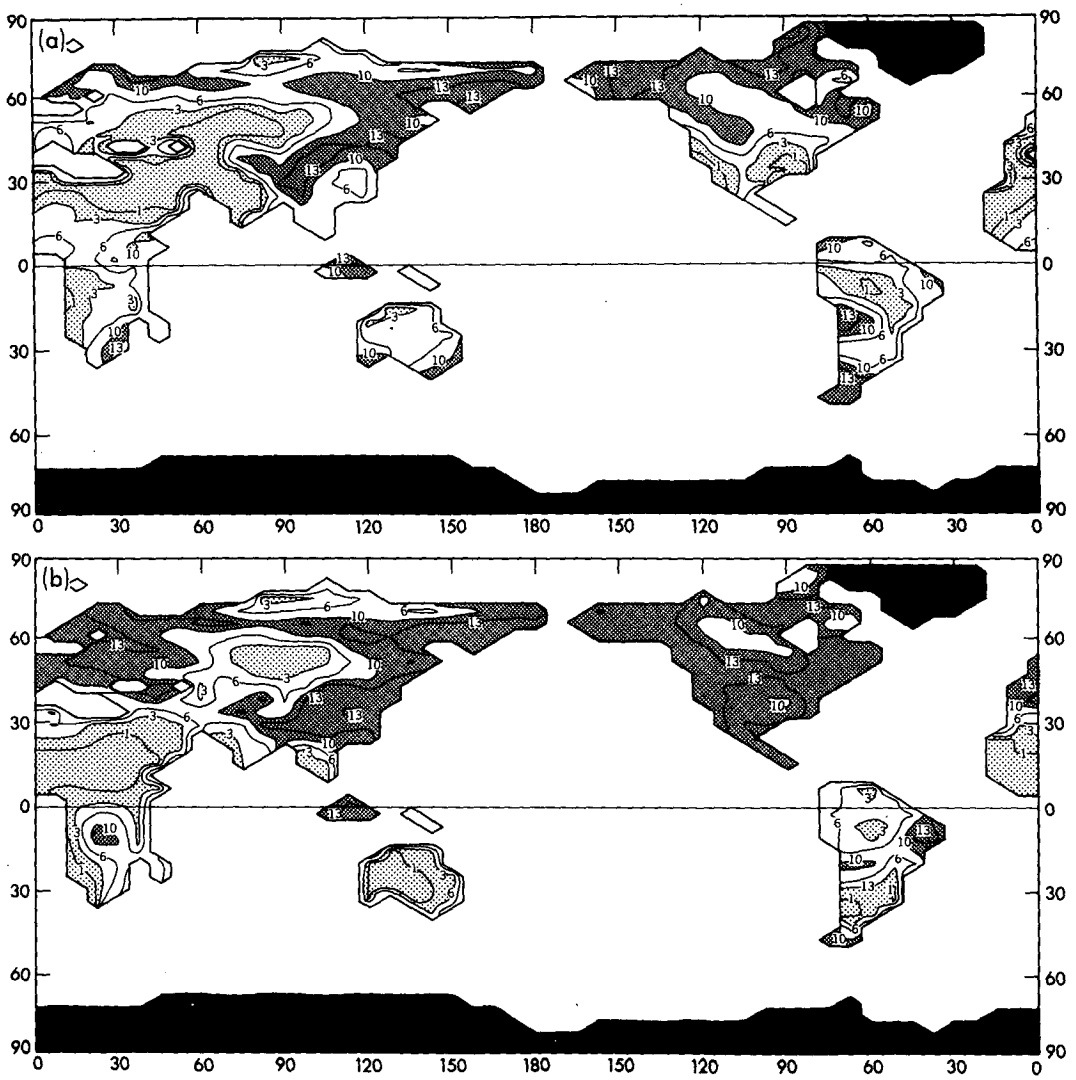

FIG. 2. Geographical distributions of soil moisture (cm) from the FC-model. (a) June–July–August, (b) December–January–February.

of the tropical rainbelt and the northeastern portion of the United States. However, the Sahara and Gobi deserts do not extend far enough southwards. In addition, Brazil and the southeastern portion of the United States are too dry during this season.

Turning to the December–January–February distribution, one may note the major arid regions in the Southern Hemisphere such as Australia and the Kalahari Desert as well as the Sahara Desert are much more extended during this period. In this season, Europe, southeast Asia and the entire North American continent are depicted as being quite wet.

Because of the absence of global observations of soil moisture, it is difficult to quantitatively assess the accuracy of the simulated distributions just illustrated. Although these distributions contain many unrealistic features, the model appears to reproduce our impression of the gross qualitative features of the global distribution of soil moisture and its seasonal variation.

3. Plan for the numerical experiments

Two series of numerical integrations are conducted by use of both FC and VC models to investigate the climatic influence of the increase in the atmospheric concentration of carbon dioxide. As listed in Table 1, the first series consists of the three integrations of the FC model in which the CO_2-concentration of the atmosphere is assumed to be 300, 600 and 1200 ppm by volume. The second series consists of the two VC model integrations with the CO_2-concentration of 300 and 600 ppm by volume. The symbols for identification and the specifications of these experiments are listed in Table 1.

TABLE 1. List of numerical integrations conducted in the present study.

Identification	Model	Atmospheric CO_2 (ppm)	Cloud cover
1X-FC integration	FC model	300	prescribed
2X-FC integration	FC model	600	prescribed
4X-FC integration	FC model	1200	prescribed
1X-VC integration	VC model	300	predicted
2X-VC integration	VC model	600	predicted

Starting from the initial conditions of an isothermal and dry atmosphere at rest and an isothermal mixed layer ocean, a numerical time integration of each experiment is performed over the period of approximately 40 years. (The period of the integration, however, differs slightly from one experiment to another depending upon the time required for reaching the quasi-steady state). For the economy of computer time, the first 10 yr of each integration is conducted by use of "asynchronous" coupling between the atmospheric and mixed layer ocean models as described by Manabe and Stouffer (1980).

The time-mean states discussed in the following sections are obtained by time averaging the state of the model over the last 10 yr of the integration of each model. For example, the effect of the CO_2-doubling upon the climate of the FC model is explored by examining the difference between the two 10-yr mean states from the 1X-FC and 2X-FC integrations. For the convenience of discussion, this pair of integrations is identified as the Δ2X-FC experiment. In a similar fashion, the pair of 1X-VC and 2X-VC integrations are called the Δ2X-VC experiment. Table 2 specifies the notations of the three experiments.

The last column of Table 2 contains the global mean increases of surface air temperature obtained from the three experiments. This information is useful to evaluate the magnitude of change of model hydrology discussed in section 4. It is of interest that the surface air temperature of the VC-model is much more sensitive to the doubling of atmospheric carbon dioxide than the FC-model. This difference in sensitivity between the two models with and without the cloud feedback process is the subject of a separate study by the present authors.

4. Change of soil moisture

a. June–July–August

The geographical distributions of the CO_2-induced change in soil moisture from all three experiments identified in section 3 are illustrated in Fig. 3. The change represents a time average over the 3-month period of June, July and August. This figure indicates that, in summer, soil moisture in both the FC and VC models over most of the North American and the Eurasian continents is reduced in response to an increase in the atmospheric concentration of carbon dioxide. As one might expect, the reduction of soil moisture in the Δ4X-FC experiment is significantly larger than the reduction in the Δ2X-FC experiment. However, the soil moisture change from the Δ2X-VC experiment has a magnitude comparable to the change in the Δ4X-FC experiment. This is reasonable in view of the fact that the magnitude of the increase of surface air temperature in the former is comparable with that in the latter experiment. As discussed in section 5 the change in soil moisture depends very much upon the magnitude of surface warming and its latitudinal variation.

Over North America one can identify a large mid-continental region of soil moisture reduction in the results from all three sets of experiments. In the Δ2X-VC experiment, the reduction occurs in a wide belt around the United States-Canadian border and another zonal belt extending from norhtern Canada to Alaska. However, these two belts are merged with each other and form one large area of soil moisture reduction in the Δ2X-FC and Δ4X-FC experiments.

Over most of the Eurasian Continent, soil moisture is also reduced in the results from all three experiments. The reduction is particularly pronounced over most of Siberia and southern Europe. In the southern part of the Eurasian Continent (i.e., the Middle East, the Indian subcontinent and Southeast Asia), the CO_2-induced change of soil moisture changes sign from one experiment to another. This is partly attributable to the large temporal variability of precipitation in these regions. Further extension of the analysis period is required to obtain more consistent results.

The statistical significance of the CO_2-induced changes of soil moisture just described is evaluated by performing the "student-t" test. At each grid point the test is applied to two sets of soil moisture data obtained from the normal and above normal CO_2-integrations. Each set consists of ten values of summer soil moisture which represent an arithmetic mean of 90 daily data. The results from this test are illustrated in Fig. 4 where the slanted shades identify the regions of statistically

TABLE 2. Identification of three experiments and their notations. The last column tabulates the differences in global mean surface air temperature (°C) between two integrations in each experiment.

Identification	Difference	Difference in global mean surface–air temperature (°C)
Δ2X-FC experiment	2X-FC minus 1X-FC integrations	2.3°C
Δ4X-FC experiment	4X-FC minus 1X-FC integrations	4.5°C
Δ2X-VC experiment	2X-VC minus 1X-VC integrations	4.0°C

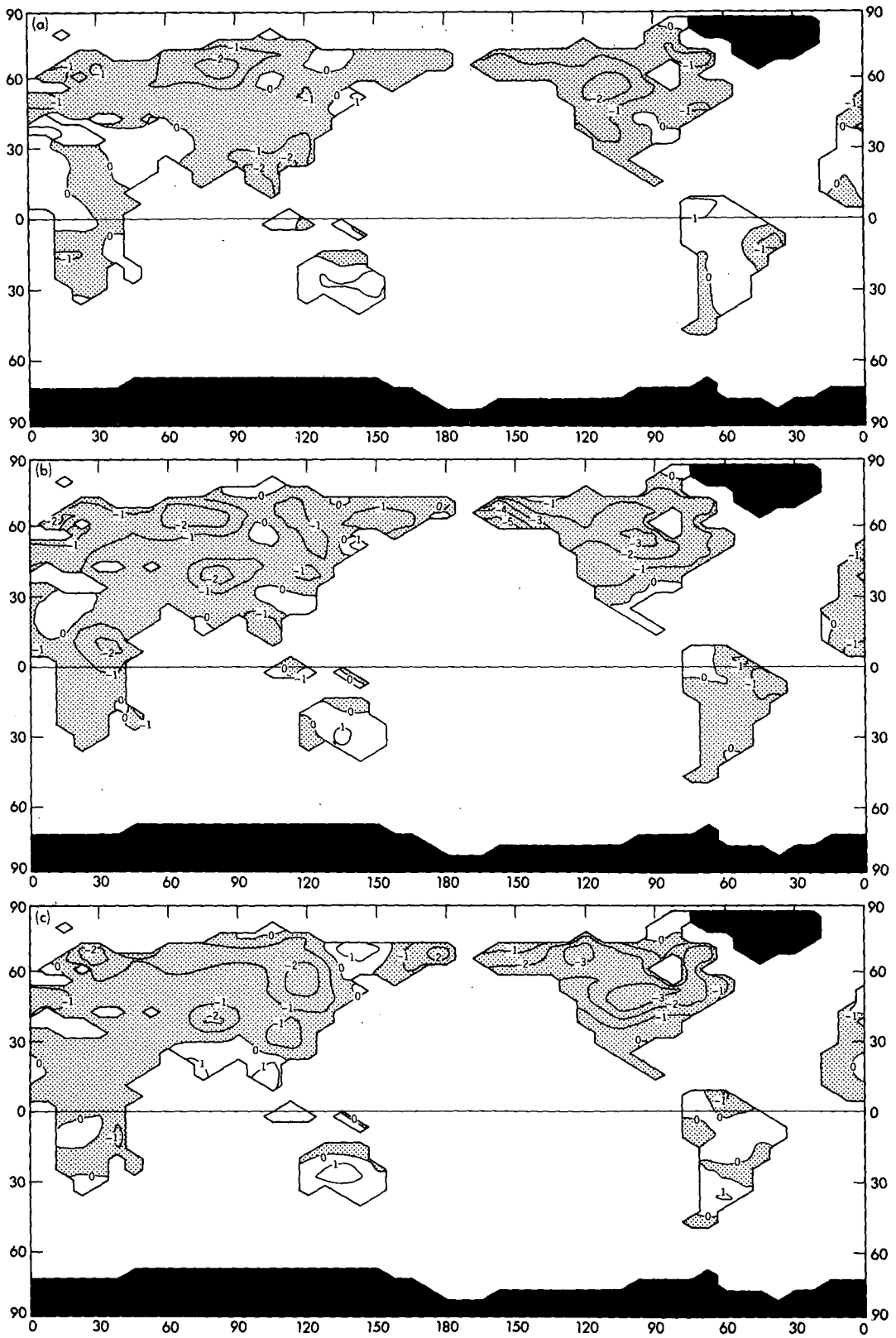

FIG. 3. The geographical distributions of the difference in soil moisture (cm) between the high CO_2- and the normal CO_2-experiments for June–July–August period. The regions of negative change are shaded. (a) Δ2X-FC experiment, (b) Δ4X-FC experiment and (c) Δ2X-VC experiment.

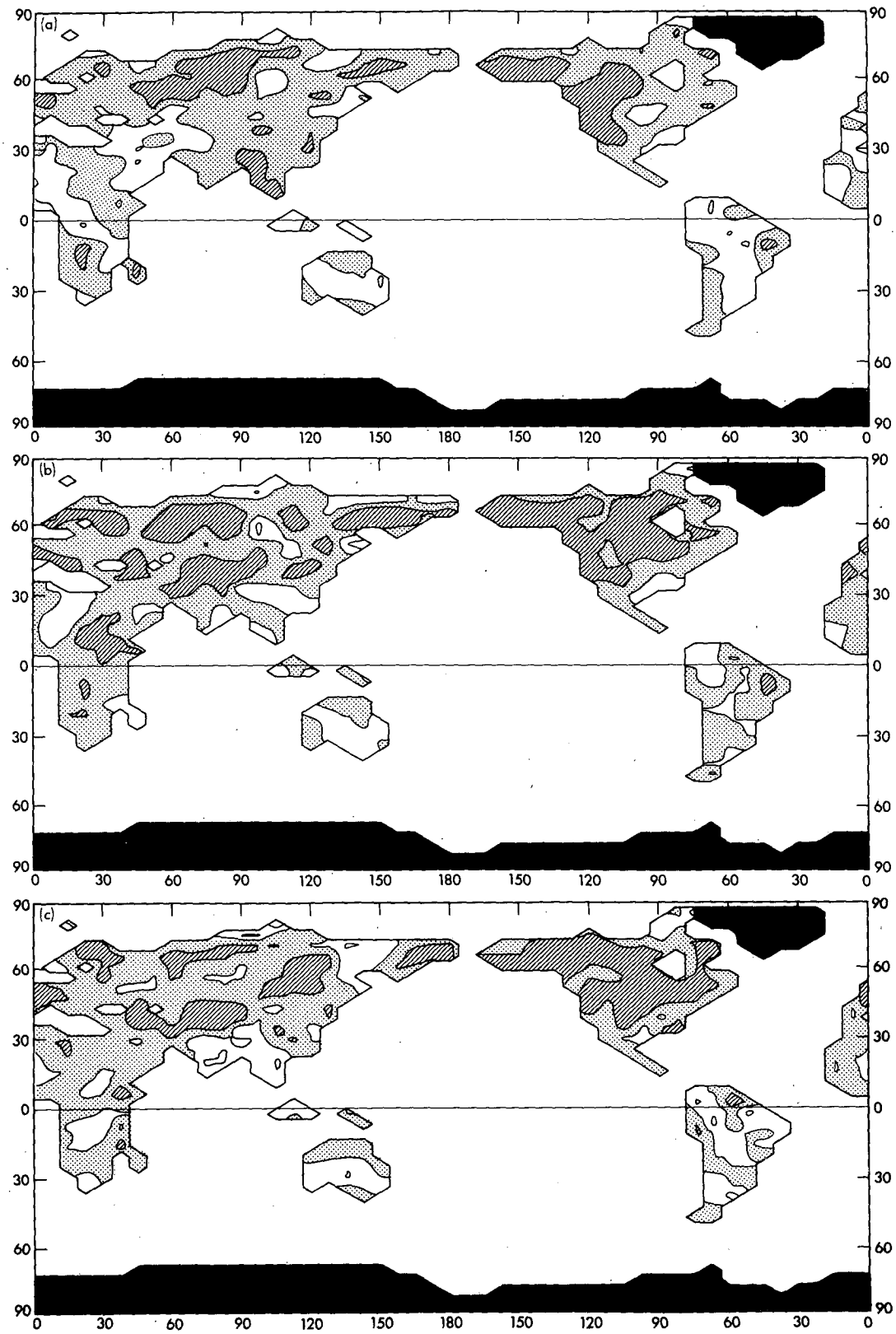

FIG. 4. The statistical significance of the CO_2-induced change in soil moisture shown in Fig. 3. Slanted areas denote regions where the negative soil moisture changes are statistically significant on the 10% level, respectively. (a) Δ2X-FC experiment, (b) Δ4X-FC experiment and (c) Δ2X-VC experiment.

significant soil moisture reduction at the 10% level. (This implies that the probability of falsely rejecting the null Hypothesis of no soil moisture change is 10% or less.) According to this figure, the reduction over North America, southern Europe and Siberia has a relatively high statistical significance. Although the reduction of soil moisture in the semiarid region located near the southern boundaries of the Iranian and Gobi Deserts is statistically significant (at the 10% level) in the Δ4X-FC and Δ2X-FC experiments, it is not significant in the Δ2X-FC experiment. This is probably due to the relatively small CO_2-induced warming in this experiment.

To appreciate the practical implication of the CO_2-induced change of soil moisture described in the preceding paragraphs, it is desirable to compare the change (ΔW) with soil moisture (W) itself by computing the percentage change of soil moisture (i.e., $100 \times \Delta W/W$). Figure 5 illustrates the geographical distributions of the percentage change of soil moisture from all three experiments. According to this figure, the maximum percentage change of soil moisture over the midcontinental region of North America is as much as 30, 40, and 50% in the results of the Δ2X-FC, Δ4X-FC and Δ2X-VC experiments, respectively. Over Siberia, it also amounts to as much as 40% in all three experiments though the geographical location of the maximum fractional change varies from one set of experiments to another. These results suggest that the change in soil moisture due to the doubling of atmospheric carbon dioxide can amount to a substantial fraction of the value of soil moisture over the midcontinental regions of North America, Siberia and Europe in summer.

b. *December–January–February*

During the December–January–February period, the CO_2-induced changes of soil moisture in the Northern Hemisphere of both models are completely different from the change for the June–July–August period described in the preceding subsections. Fig. 6 illustrates the geographical distributions of the change of soil moisture from the three sets of experiments. This figure indicates that, in all experiments, soil moisture increases with increasing atmospheric carbon dioxide over most of the North American and the Eurasian continent poleward of 30°N. On the other hand, soil moisture decreases in most of the subtropical belt ranging from 20° to 30°N in the results of all three sets of experiments.

The maps in Fig. 7 identifies the regions where the CO_2-induced changes of soil moisture during the December–January–February period are statistically significant at the 10% level. According to this figure, the increases of soil moisture in the middle and high latitude-portions of both the North American and Eurasian continents are statistically significant at the 10% level in the results from the Δ4X-FC and Δ2X-VC experiments. The corresponding increase of soil moisture in the Δ2X-FC experiment has a somewhat lower statistical significance though one can identify the narrow patches of the areas where the change is significant at the 10% level. Nevertheless, the patterns of the CO_2-induced increase of soil moisture in western and northeastern Siberia and the Mackenzie River Basin of Canada from the three experiments are qualitatively similar to each other. This similarity enhances the reliability of the present results.

In the subtropical belt where soil moisture tends to decrease in winter in response to an increase of atmospheric carbon dioxide, the reduction in southern California and Mexico is significant at the 10% level in the results from all three experiments. Although soil moisture does not reduce in winter in the northern coast of Africa in the Δ2X-VC experiment, it does in both Δ2X-FC and Δ4X-FC experiments. This reduction in the latter two experiments is statistically significant at the 10% level. The winter reduction of soil moisture over India is statistically significant at the 10% level in the Δ2X-FC experiment but is not in the other two experiments. Further extension of the period for the numerical time integrations of the climate models may be necessary to get more consistent results from all three experiments. Nevertheless, the results from the present study reveal the tendency of both FC and VC models to reduce soil moisture in the subtropics during winter in response to an increase of CO_2 concentration of the atmosphere. This tendency is evident in the CO_2-induced change in zonal mean soil moisture described in the following subsection.

c. *Zonal mean change*

The latitude–month distributions of the CO_2-induced changes of zonal mean soil moisture from the three sets of experiments are illustrated in Fig. 8. The results from all three experiments show that soil moisture in middle and high latitudes of the Northern Hemisphere is reduced in summer whereas it increases in winter. In the subtropics, soil moisture tends to reduce in winter in response to an increase of CO_2 concentration of the atmosphere.

The distribution of soil moisture change previously described is in qualitative agreement with the distribution which was obtained from the earlier study of Manabe et al. (1981) and was discussed extensively in a review paper by Manabe and Wetherald (1985). It is also similar to the results from the study of Mitchell and Lupton (1984) which was briefly described in the Introduction of this paper. The present result, however, differs from that of Washington and Meehl (1984) which indicates an increase of zonal mean soil moisture throughout the year in middle latitudes of the Northern Hemisphere, although the magnitude of the increase in summer is considerably less than that in winter. Hansen et al. (Mitchell and Schlesinger, 1986) obtained a zonal mean change of soil moisture which is

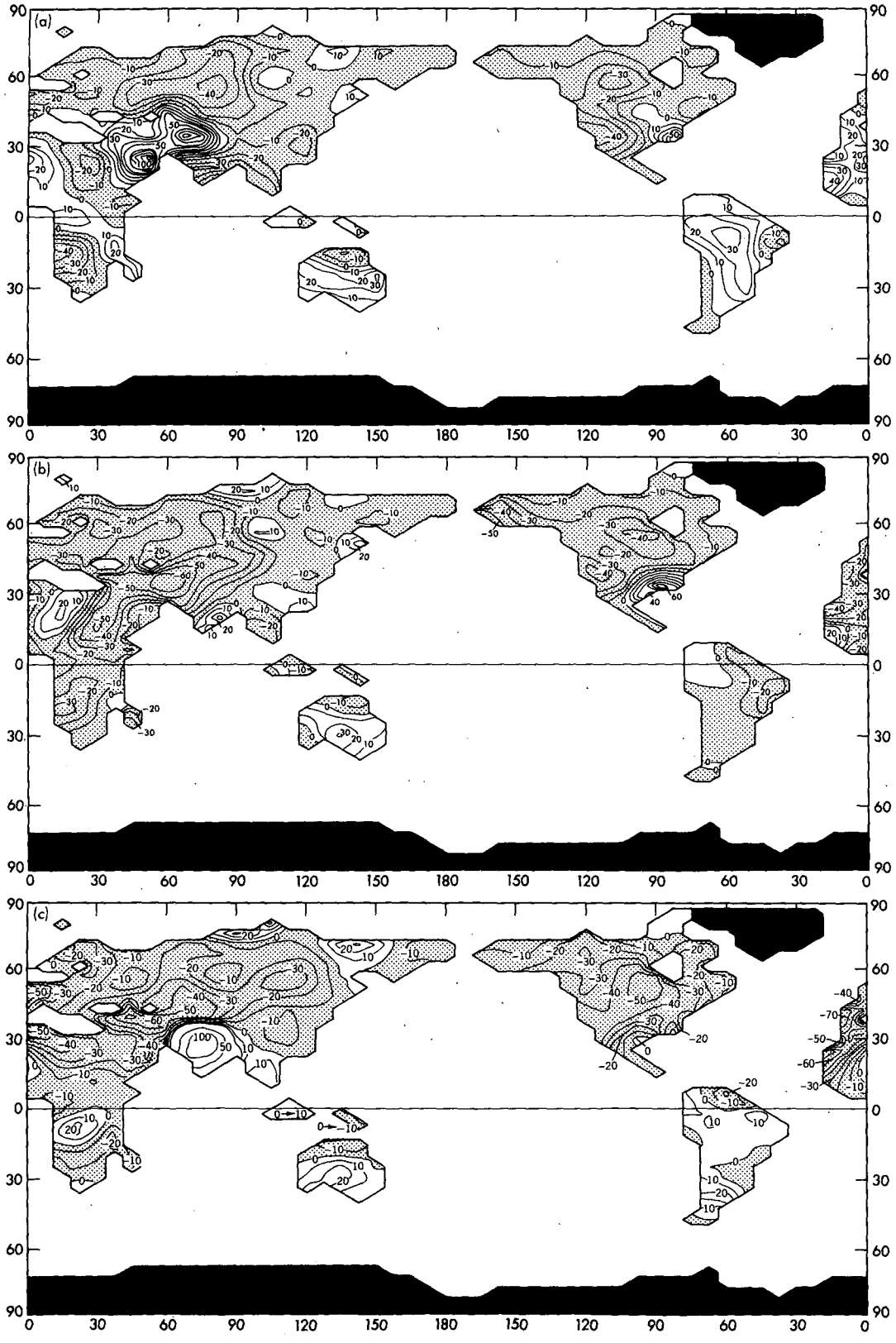

FIG. 5. The geographical distribution of the percentage difference in soil moisture between the high CO_2- and the normal CO_2-cases for June–July–August period. (a) Percentage difference between 2X-FC and 1X-FC integrations, (b) percentage difference between the 4X-FC and 1X-FC integrations and (c) percentage difference between 2X-VC and 1X-VC integrations.

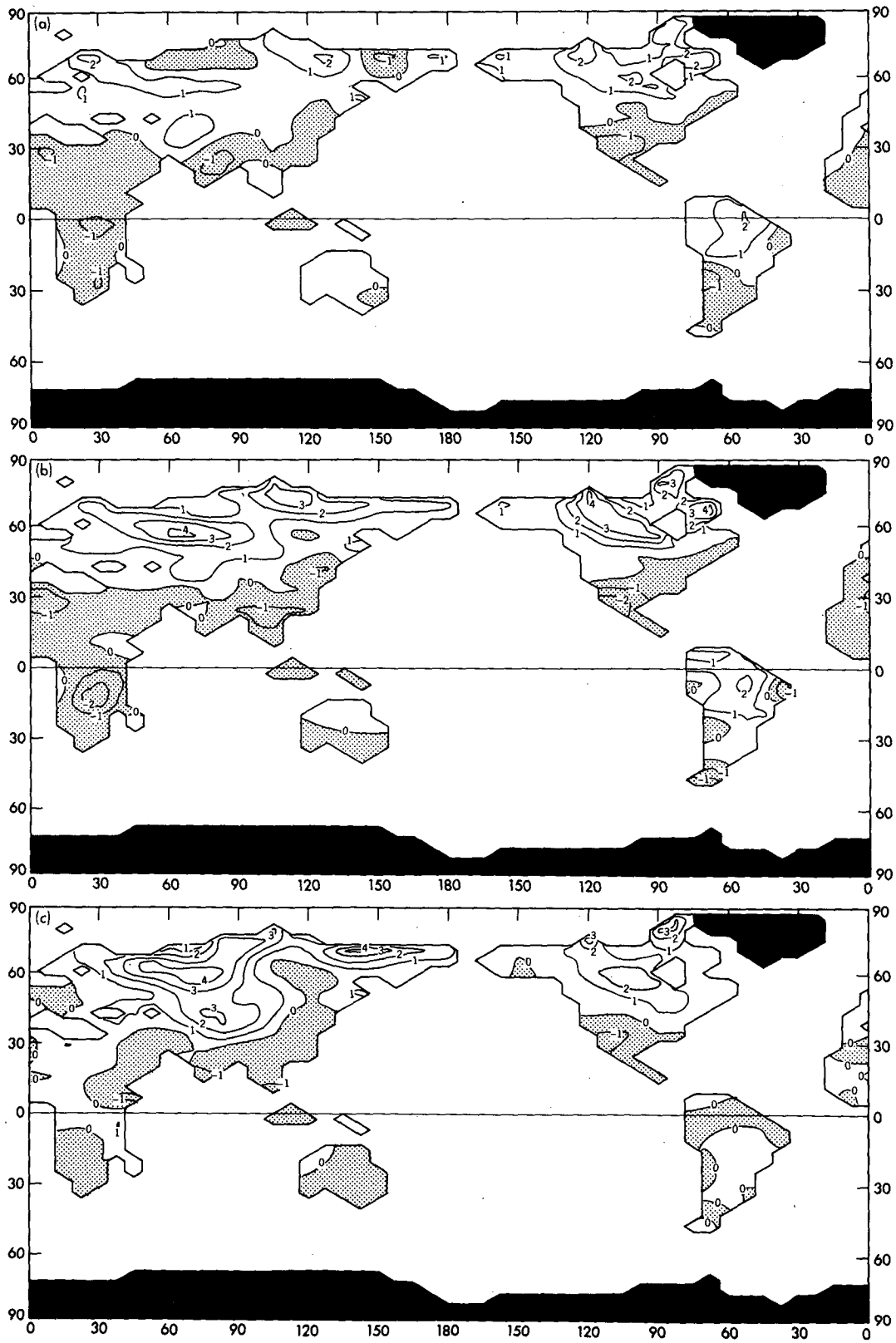

FIG. 6. As in Fig. 3 except that the figure is made for the December–January–February period.

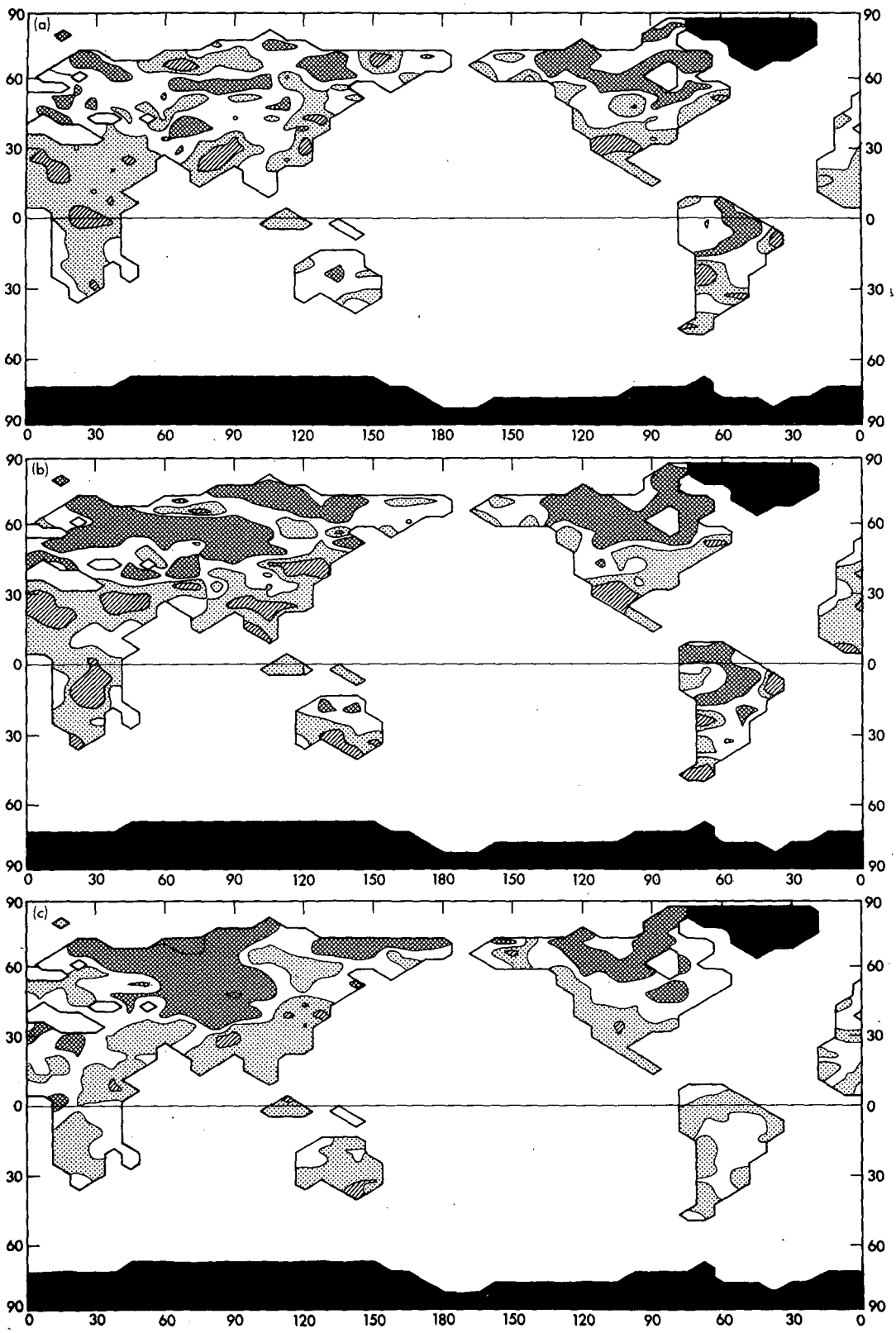

FIG. 7. As in Fig. 4 except that the figure is made for the December–January–February period. In addition, cross-hatched shading denotes regions where positive soil moisture changes are statistically significant at the 10% level.

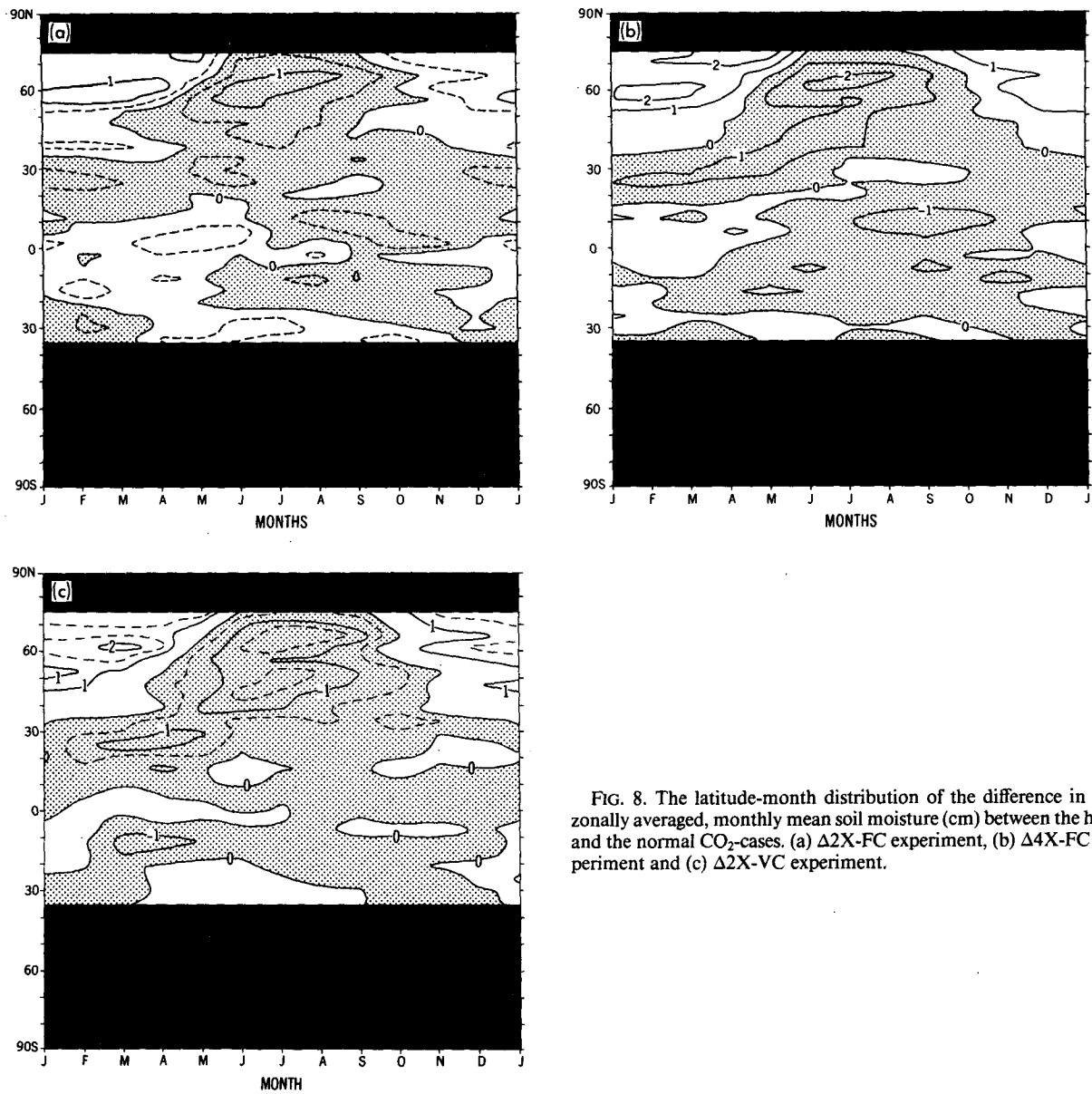

FIG. 8. The latitude-month distribution of the difference in the zonally averaged, monthly mean soil moisture (cm) between the high and the normal CO_2-cases. (a) Δ2X-FC experiment, (b) Δ4X-FC experiment and (c) Δ2X-VC experiment.

qualitatively similar to the present results. However, the magnitude of the summer reduction in their experiment is much smaller than the reductions obtained from the present experiments.

The qualitative similarity between the results from the FC- and VC-model suggests that the cloud feedback process is not necessary for inducing the CO_2-induced change of soil moisture just described. One should note, however, that the change of surface air temperature of the VC-model in response to the doubling of atmospheric carbon dioxide is larger than the corresponding change of the FC-model thereby inducing the larger change of soil moisture. In addition, the summer reduction of soil moisture in middle latitudes of the VC-model is enhanced further due to the reduction of cloud amount and increased potential evaporation over the continents as discussed in the section 5.

d. Southern Hemisphere

So far, the description is limited to the change of soil wetness in the Northern Hemisphere. In the Southern Hemisphere of both FC and VC models one notes narrow patches where the CO_2-induced change has statistical significance with confidence level of 10% or higher. Unfortunately, these changes are not necessarily common in the results from the three sets of experiments. As described previously, the CO_2-induced change of soil moisture in middle and high latitudes of the Northern Hemisphere changes sign from winter

to summer. This is because the surface water budget and its CO_2-induced change depend strongly upon season as discussed in section 5. However, in the Southern Hemisphere where the continents are narrow and the seasonal variation of surface air temperature is relatively small, the CO_2-induced change of soil moisture is expected to be less pronounced and less detectable than in the Northern Hemisphere. Thus, it is not surprising that the changes of soil moisture in the Southern Hemisphere vary from one experiment to another. Because of these inconsistencies, the CO_2-induced change in the Southern Hemisphere is not discussed in the present study.

5. Budget analysis of water and heat

To investigate the mechanisms which are responsible for the CO_2-induced changes of soil moisture described in section 4, a detailed analysis of the water and heat budgets are performed over four continental regions for both FC- and VC-models. The regions selected are 1) northern Canada, 2) Great Plains of North America, 3) southern Europe and 4) northern Siberia. The geographical domains of these regions are specified in the map of Fig. 9. The size of each region is chosen to be small enough so that the physical mechanisms responsible for the CO_2-induced change of soil moisture do not differ substantially from one part of the region to another. At the same time, it is large enough to distinguish the CO_2-induced change of area mean moisture from its natural variability.

Before proceeding to the discussion of water budgets at the four specific continental regions just identified, it is convenient to identify various components of the surface water balance which contribute to the change of soil moisture. The prognostic equation of soil moisture (W) may be written as

$$\partial W/\partial t = r - e + m - f \qquad (1)$$

where r, e, m, and f are area mean rates of rainfall, evaporation, snowmelt, and runoff, respectively; t is time. The area averaging was performed over each of the four regions selected for analysis. To evaluate the seasonal variation of the CO_2-induced change of soil moisture of the model, one can also use the prognostic equation of the difference in soil moisture between the normal and high CO_2 cases, i.e.,

$$\partial \Delta W/\partial t = \Delta r - \Delta e + \Delta m - \Delta f \qquad (2)$$

where, for example, ΔW denotes the excess of soil moisture in a high CO_2 case over the soil moisture in the normal CO_2 case. Equations (1) and (2) contain all the components of the water balance to be considered in the following discussions. Beginning with northern Canada, the water budgets of all four regions selected above is the subject of the following discussion.

a. Northern Canada

The FC-Model. Fig. 10a compares the annual variations of soil moisture over Northern Canada from the 4X- and 1X-FC integrations. In both cases the soil is almost saturated with water in spring but becomes drier towards summer. After August, soil moisture increases with time and reaches high winter values by the end of November.

During winter, soil moisture from the 1X-FC integration is significantly less than that from the 4X-FC integration. However, the former becomes more than

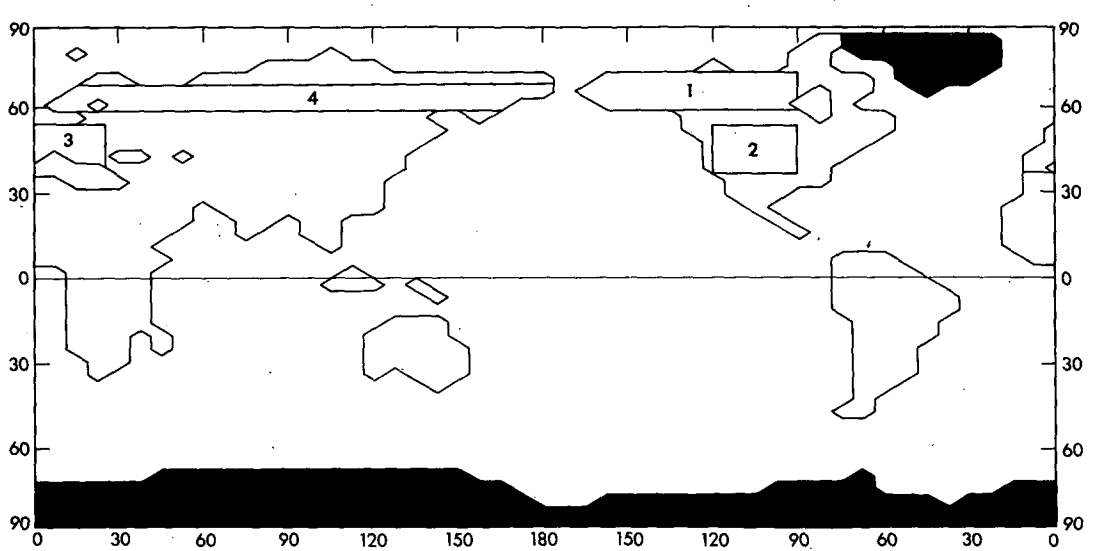

FIG. 9. The map which depicts the four regions chosen for detailed analysis. Region 1: northern Canada; Region 2: Great Plains of North America; Region 3: southern Europe; and Region 4: northern Siberia.

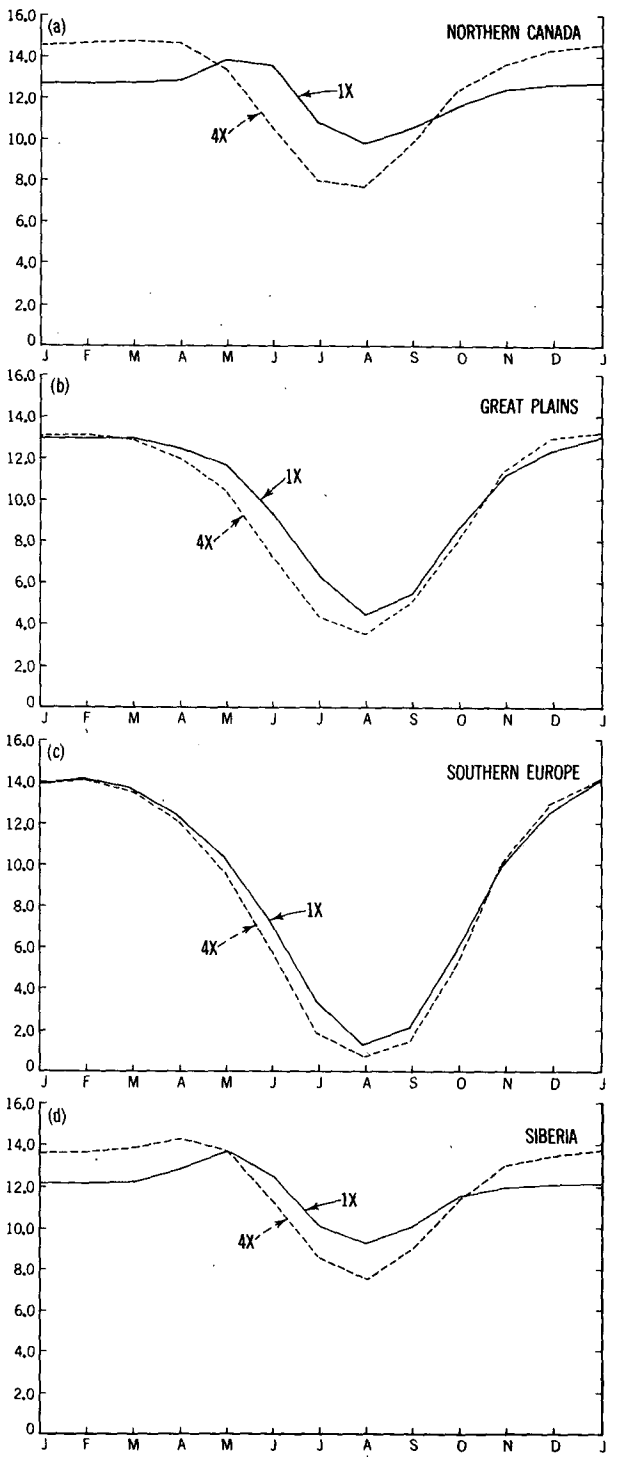

FIG. 10. Seasonal variation of area mean soil moisture (cm) in four selected regions of the FC model: (a) northern Canada, (b) Great Plains of North America, (c) southern Europe and (d) northern Siberia. Solid lines: 1X-FC integrations; dashed lines: 4X-FC integration.

the latter as the season proceeds from spring to summer. In other words, the soil in northern Canada of the FC-model becomes wetter in winter and dryer in summer in response to the quadrupling of the atmospheric CO_2-concentration.

To investigate the physical mechanism responsible for the CO_2-induced change in the seasonal variation of soil moisture over the region of northern Canada, Fig. 11 is constructed. This figure illustrates the seasonal variation of various water balance components obtained from the 1X- and 4X-FC runs. The components of the water balance shown here appear in the right-hand side of Eq. (1) and are r, $-e$, m, and $-f$. The

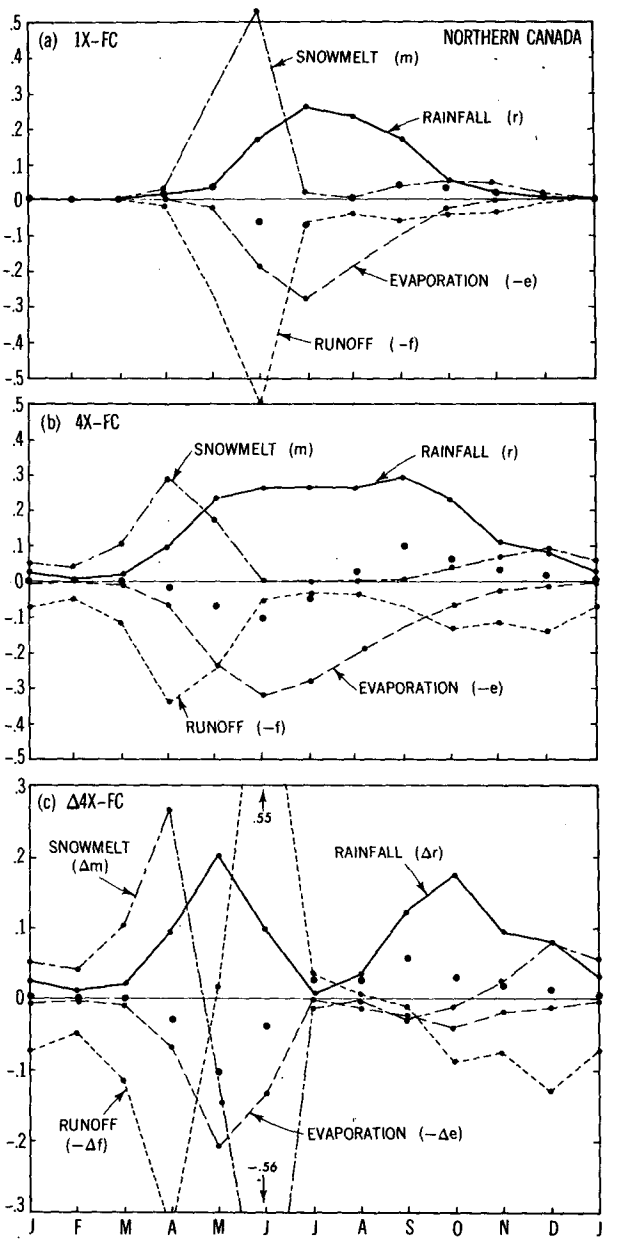

FIG. 11. Seasonal variation of surface water budget averaged over the northern Canadian region of the FC model. (a) 1X-FC integration; (b) 4X-FC integration; (c) 4X- minus 1X-FC integrations. Large dots indicate $\partial W/\partial t$ in (a) and (b) and $\partial \Delta W/\partial t$ in (c). Units are in cm day^{-1}.

minus sign is added to e and f because evaporation and runoff constitute the loss of water from the continental surface. In the bottom of this figure, the annual marches of the differences in these water balance components in the right-hand side of Eq. (2) are illustrated to examine the CO_2-induced change in the surface water budget.

Examining the results from the 1X-integration shown in the top of Fig. 11, one notes that both snowmelt and runoff are at a maximum in June when soil is nearly saturated with water. After the snowmelt season, the continental surface is free of snow cover. Thus, a larger fraction of insolation reaching the continental surface is absorbed and becomes available for evaporation. The enhanced evaporation contributes to the reduction of soil moisture as the season progresses from spring to summer.

When one compares the results from the 1X-FC integration previously described with those from the 4X-FC integration, one notes a significant difference in the timing and intensity of snowmelt in spring. To appreciate this difference, it is desirable to examine Fig. 12 which illustrates the seasonal variation of rainfall, snowfall, precipitation and snowmelt from both integrations. This figure indicates that, in the 1X-FC case, practically all precipitation takes place as snowfall and very little snowmelt occurs during winter and early spring. On the other hand, in the warmer 4X-FC case, the snowfall fraction (i.e., the fraction of precipitation which falls as snow) is significantly less than 1 and some snowmelt occurs throughout winter followed by the rapid reduction of snowfall fraction and increase of snowmelt in early spring. Thus, the snowfall season is shorter and the total snow accumulation during the cold period is smaller in the 4X- as compared with the 1X-FC case. The difference in the intensity and timing of snowmelt in spring manifests itself in Fig. 11c as a large negative difference in June contributing to the earlier commencement of the spring to summer reduction of soil moisture in the 4X-FC integration.

Another consequence of the earlier arrival of the snowmelt season in the 4X-FC integration is the earlier disappearance of snowcover in spring. Since snow cover with a large surface albedo prevents the absorption of solar energy by a continental surface and reduces the rate of potential evaporation, the earlier disappearance of snow cover enhances evaporation during the months of April, May and June. As Fig. 11 indicates, the combined effects of the decreased snowmelt and the enhanced evaporation overcome the effect of the increase in precipitation, thus decreasing soil moisture and runoff in the late spring and early summer, respectively. Thus, the spring-to-summer reduction of soil moisture begins earlier, resulting in the CO_2-induced reduction of soil moisture in summer.

As noted earlier, the soil wetness of the FC model is enhanced during winter in response to the quadrupling of the atmospheric carbon dioxide. Because of a high surface temperature, the rainfall season (i.e., the period when precipitation consists mostly of rainfall)

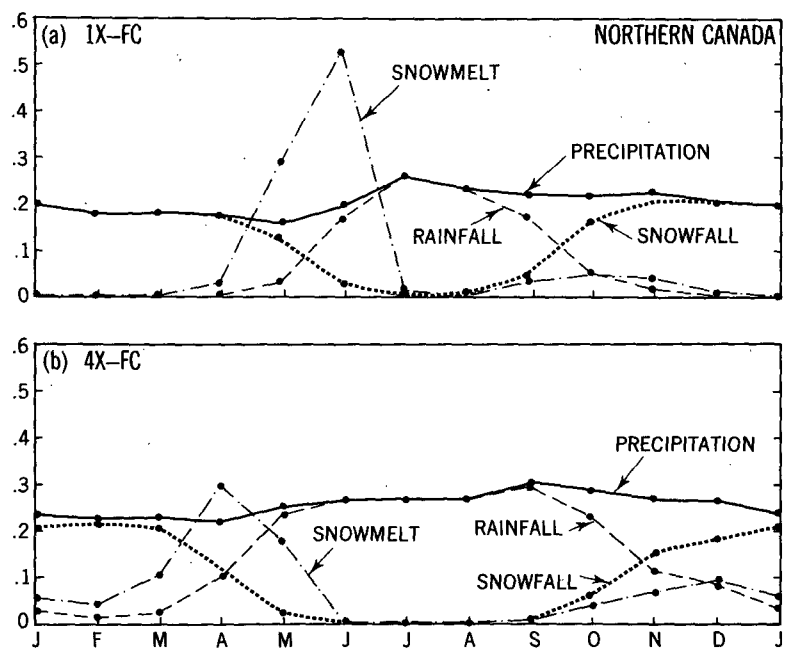

FIG. 12. Seasonal variation of the rates of rainfall (dashed line), snowfall (dotted line), precipitation (solid line) and snowmelt (dash-dotted line) averaged over the northern Canadian region of the FC. Here, precipitation is the sum of rainfall and snowfall. (a): 1X-FC integration and (b) 4X-FC integration. Units are in cm day^{-1}.

lasts longer and ends later during fall in the 4X-FC case increasing soil wetness during winter. This is clearly indicated in Fig. 12. In addition, both snowmelt and rainfall are larger during winter in the 4X-FC integration enhancing further the soil wetness. This CO_2-induced increase in rainfall during fall and winter is attributable not only to a larger rainfall-fraction (i.e., the ratio of rainfall to total precipitation) but also to the overall rise in precipitation rate. The increase of precipitation rate results from the penetration of warm, moisture-rich air into high latitudes where the CO_2-induced warming is relatively large. In short, soil wetness is enhanced in winter due to the increase in both rainfall and snowmelt during fall and winter.

The VC-Model. The seasonal variations of soil moisture and various components of water balance over northern Canada of the VC-model are also qualitatively similar to those of the FC-model, indicating the similarity of the mechanism responsible for the soil moisture change in the two models. However, the magnitude of the soil moisture change in the VC-model in response to the doubling of the atmospheric CO_2 is comparable to that of the FC-model in response to the CO_2-quadrupling. These results are consistent with the fact that the sensitivity of the global mean surface air temperature of the VC-model is larger than that of the FC-model (see Table 2).

b. Great Plains

The FC-Model. According to Fig. 10b, soil over the Great Plains region of the FC-model is nearly saturated with water during winter, but rapidly loses moisture after spring. In summer, the soil of the Great Plains is much drier than the soil of northern Canada in both the 1X- and 4X-FC integrations. According to the comparison of the results from these two integrations, soil moisture over the Great Plains region of the FC-model is reduced significantly during summer in response to the quadrupling of atmospheric carbon dioxide. This is consistent with Fig. 3b which illustrates the geographical distribution of the CO_2-induced change of soil moisture of the FC-model in summer.

To investigate the physical mechanisms responsible for the summer reduction of soil moisture previously mentioned, graphs illustrating the seasonal soil moisture budget of the Great Plains are constructed for both 1X- and 4X-FC runs and are shown in Figs. 13a, b, respectively. The comparison of these two figures reveals that the snowmelt season of the 4X-FC case ends earlier than the 1X-FC case. Because of the earlier termination of the snowmelt season, the availability of snowmelt-water in the 4X-FC case is less than the 1X-FC case in April and May (see Fig. 13c which illustrates the difference in seasonal water budget between the two cases). Furthermore, the earlier disappearance of snow cover enhances evaporation and reduces soil moisture in late spring. Both reduced snowmelt and enhanced evaporation in the late spring contribute to

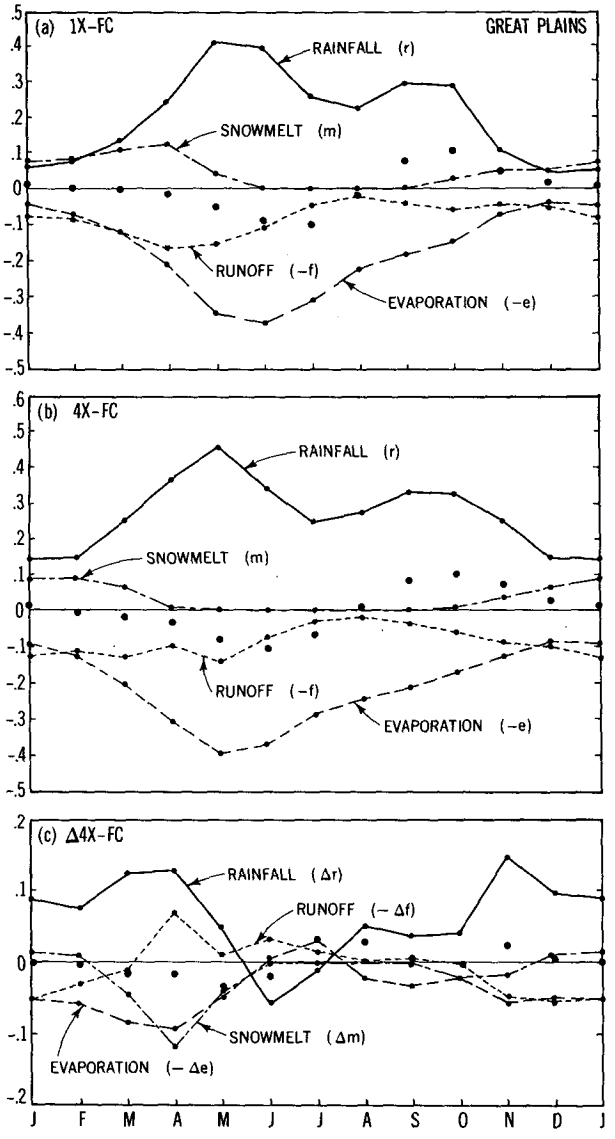

FIG. 13. Seasonal variation of surface water budget averaged over the Great Plains region of the FC-model. (a) 1X-FC integration, (b) 4X-FC integration and (c) 4X- minus 1X-FC integration. Large dots indicate $\partial W/\partial t$ in (a) and (b) and $\partial \Delta W/\partial t$ in (c). Units are in cm day^{-1}.

the earlier commencement of the reduction of soil moisture from spring to summer and are responsible for the CO_2-induced summer reduction of soil moisture over the Great Plains in the FC-model.

To appreciate the seasonal variation of the surface water budget previously described, it is useful to examine the seasonal variation of the surface heat balance. Since it is assumed that the land surface has no heat capacity, the equation of surface heat balance over a continental surface may be written as

$$\mathrm{DSR} - \mathrm{ULR} - \mathrm{SH} - \mathrm{LH} - \mathrm{LM} = 0$$

where DSR is net downward solar radiation; ULR, net upward long wave radiation; SH, upward flux of sen-

sible heat; LH, upward flux of latent heat; and LM latent heat of melting. The equation for the CO_2-induced change in surface heat balance can be written as

$$\Delta DSR - \Delta ULR - \Delta SH - \Delta LH - \Delta LM = 0$$

where Δ denotes the difference between the high and normal CO_2-experiments.

The annual marches of the difference in various heat balance components between the 1X- and 4X-FC integrations are illustrated in Fig. 14 for the Great Plains region. Owing to the reduction of surface albedo resulting from the early disappearance of snowcover, the surface absorption of solar radiation over the Great Plains region increases markedly in winter and early spring in response to the quadrupling of the atmospheric carbon dioxide. In addition, the heat available for the surface of the Great Plains increases in spring because of the reduction of latent heat required for melting snow cover. Other heat gains include the increase in the downward flux of terrestrial radiation caused by the rise in the concentrations of CO_2 and H_2O in the model atmosphere. These CO_2-induced heat gains enhance the evaporation from the Great Plains in spring contributing to the reduction of soil moisture as described in the preceding paragraph.

The consequence of the early termination of the snowmelt season described before is qualitatively similar to the situation over northern Canada. However, there are other factors which also contribute to the reduction of soil moisture over the Great Plains in summer. One such factor is the change of precipitation. As indicated in many numerical experiments conducted earlier (e.g., Manabe and Wetherald, 1975; Manabe and Stouffer, 1980; Washington and Meehl, 1984), the CO_2-induced warming in the lower troposphere of the present model increases with increasing latitudes. Therefore, in the high CO_2-(4X-) atmosphere, the warm air with a relatively high concentration of water vapor can penetrate into higher latitudes than the normal CO_2-(1X-) atmosphere. Thus, the rate of precipitation increases markedly in the northern half of the middle latitude rainbelt, whereas it hardly increases (or decreases slightly) in the southern half of the rainbelt despite the increase in global mean precipitation. This is indicated in Fig. 15 which illustrates how the seasonal and latitudinal distribution of precipitation over the Great Plains is altered in response to the quadrupling of the atmospheric concentration of carbon dioxide. (A qualitatively similar change in precipitation rate occurs at other longitudes. The CO_2-induced change of poleward moisture transport in the model atmosphere is the subject of further discussion in the Appendix.) Because of the poleward shift of the rainbelt from winter to summer, a middle latitude location, which is situated under the northern part of the rainbelt in winter, will be under the southern part in summer. Therefore, the CO_2-induced change of precipitation rate at this location is rapidly reduced from a large positive to slightly negative value as the season proceeds from spring to summer. The combined effects of enhanced evaporation and reduced snowmelt exceeds the contribution from the increased rainfall and increased snowmelt resulting in the reduction of soil moisture and runoff in May as illustrated by Fig. 13c. During June and July, the CO_2-induced change of rainfall becomes negative and helps maintain the soil moisture from the 2X-integration at a lower level than the 1X-case.

Contrary to the situation in summer, the soil wetness over the Great Plains increases during winter in response to the quadrupling of atmospheric carbon dioxide. In qualitative agreement with the situation over northern Canada, this enhanced wetness results mainly from the increased rainfall during late fall and winter. In these seasons, the Great Plains are situated in the northern part of the middle latitude rainbelt where the precipitation rate increases in response to an increase

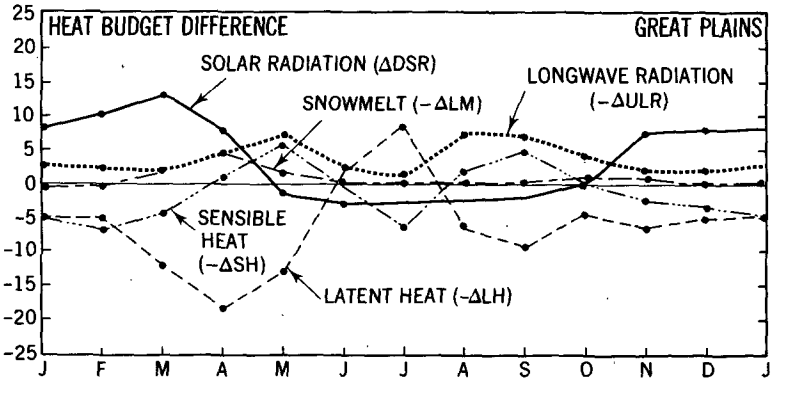

FIG. 14. Seasonal variation of the difference in surface heat budget of the Great Plains region between the 4X-FC and 1X-FC integrations. (Solid line: ΔDSR; dotted line: −ΔULR; dash-dot-dot-dotted line: −ΔSH; dashed line: −ΔLH; dash-dotted line: −ΔLM.) Units are in W m^{-2}.

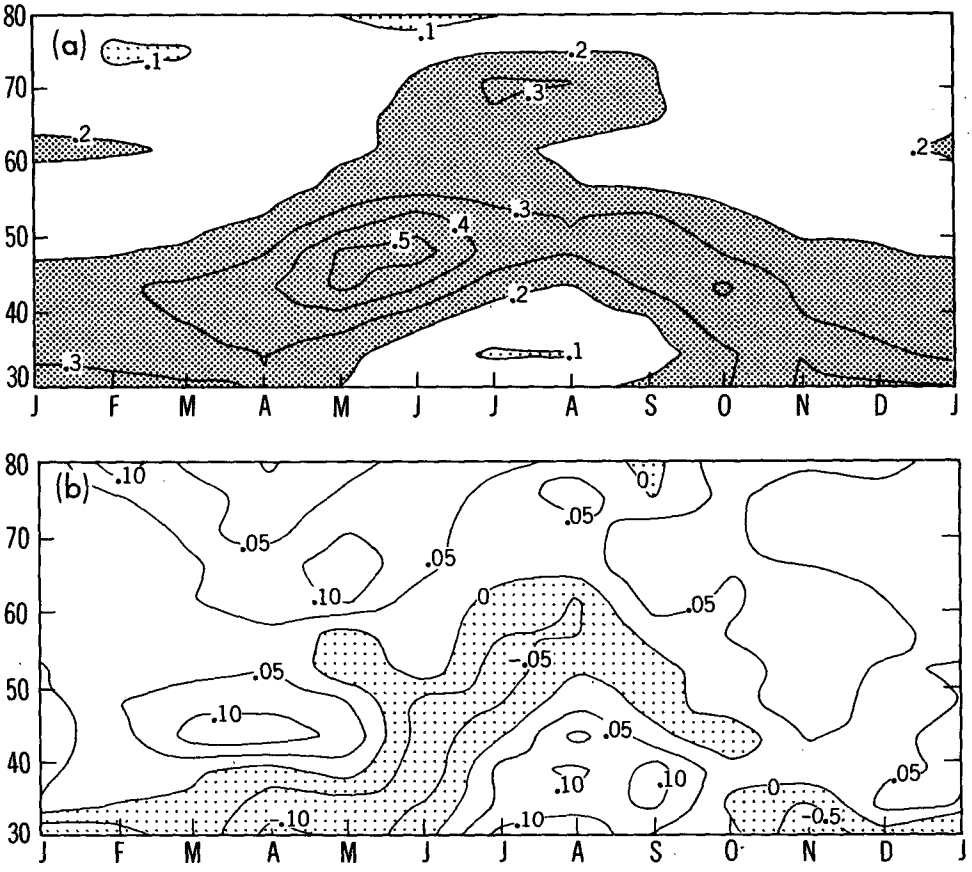

FIG. 15. The latitude month distributions of (a) zonally averaged, monthly mean rate of precipitation obtained from the 1X-FC integration and (b) the difference in zonally averaged, monthly mean rate of precipitation between the 4X-FC and 1X-FC integrations. Here, zonal mean is computed over the Great Plains of North America as identified in Fig. 9. Units are in cm day^{-1}.

in atmospheric carbon dioxide. Owing to the CO_2-warming, a larger fraction of this increased precipitation occurs as rainfall in the 4X-FC integration contributing to the increase of soil wetness previously mentioned. The changes in precipitation and rainfall as just described are clearly indicated in Fig. 16 which illustrates the annual marches of these hydrologic variables in the 4X- and 1X-FC integrations and the difference of these variables between the two integrations. Figure 13c clearly indicates that the large positive contribution from the increased rainfall overshadows all other effects in the late fall and winter maintaining the soil wetness over the Great Plains near saturation in the 4X-FC integration during these seasons.

The VC Model. The seasonal variation of soil moisture over the Great Plains region, which is obtained from both 1X-VC and 2X-VC integrations, is illustrated in Fig. 17a. In agreement with the behavior of the FC model, the area mean values of soil moisture over the Great Plains are close to saturation in winter and are reduced towards summer. In both VC integrations, the summer values of soil moisture are significantly lower than the corresponding values from the FC experiments. A comparison of Fig. 17a with Fig. 10b reveals that, in July, the difference in soil moisture between the 2X-VC and 1X-VC integrations is substantially larger than the difference between the 4X-FC and 1X-FC integrations. The large sensitivity of soil wetness over the Great Plains of the VC model in summer is the subject of the discussion in this subsection.

The seasonal variation of the differences in various components of the surface water budget between the 2X-VC and 1X-VC integrations are illustrated in Fig. 17b for the Great Plains region. Although this figure resembles Fig. 13c from the FC model, it possesses some distinct features. For example, the difference in rainfall rate between the two runs acquires a large negative value in June and remains negative throughout summer. In other words, the rate of rainfall over the Great Plains of the VC model is reduced substantially during summer in response to the doubling of atmospheric carbon dioxide. Although the difference in rainfall rate also becomes negative during June and July over the Great Plains of the FC model as shown

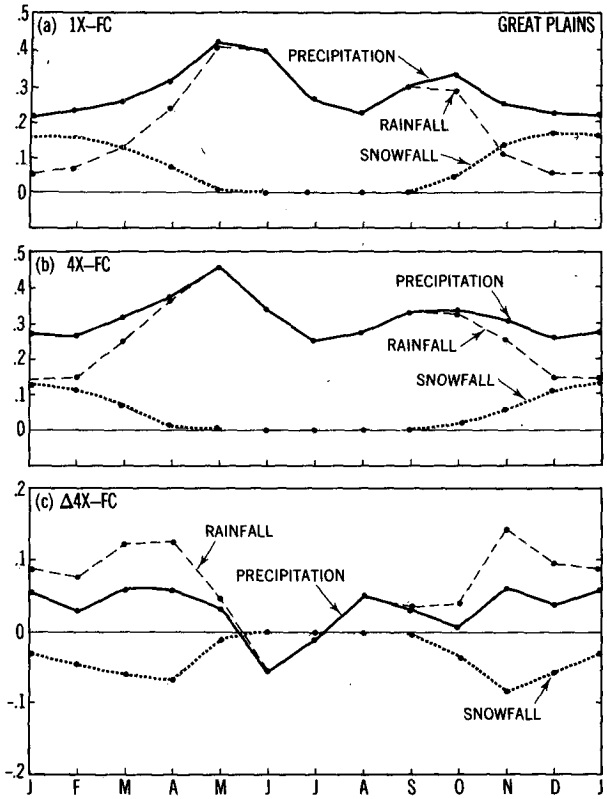

FIG. 16. Seasonal variation of the rates of rainfall (dashed line), snowfall (dotted line), and precipitation (solid line) averaged over the Great Plains region, North America of the FC model. (a): 1X-FC integration, (b) 4X-FC integration and (c) 4X minus 1X-FC integration. Units are cm day^{-1}.

in Fig. 13c, its magnitude is much smaller. The large CO_2-induced reduction of rainfall previously described contributes to the reduction of soil moisture over the Great Plains in summer. This reduction of rainfall is further enhanced by the positive feedback mechanism involving cloud cover as described below.

When the soil moisture over a continent is reduced, the ventilation of the radiation energy received by a continental surface is accomplished by the upward flux of sensible rather than latent heat. Thus, the temperature of the continental surface and lower troposphere increases. The warming over the Great Plains region is clearly indicated in Fig. 18a which illustrates the geographical distribution of the change in the surface air temperature of the VC model for the period of June–July–August in response to the doubling of the atmospheric carbon dioxide. Such a warming, in turn, reduces both the relative humidity of the lower troposphere and the rate of precipitation. The reduction of relative humidity is also accompanied by the reduction of cloud amount which increases the solar energy reaching the continental surface. A substantial reduction of cloud amount is clearly indicated in Fig. 18b which illustrates the geographical distribution of the change in cloud amount of the VC model in response to the CO_2 doubling. The increased availability of solar energy at the continental surface enhances the ventilation through upward fluxes of sensible and latent heat. Both the reduction of precipitation and the increase of radiation energy available at the surface contribute to further reduction of soil wetness over the Great Plains of the VC model in summer.

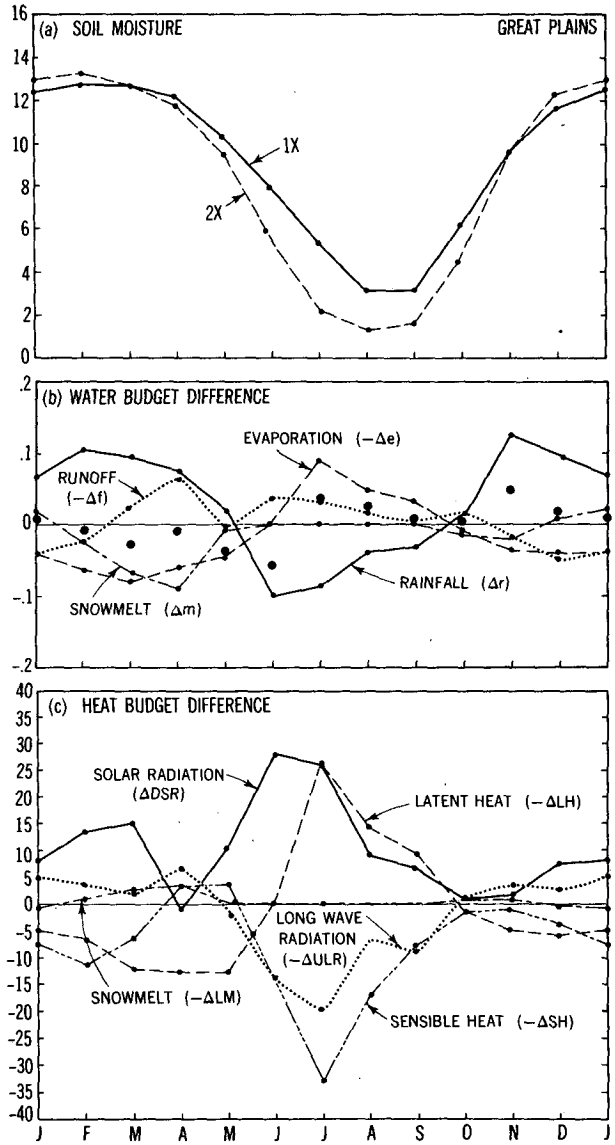

FIG. 17. (a) Seasonal variation of soil moisture (cm) averaged over the Great Plains region of the VC-model. Solid line: 1X-VC integration; and dashed line: 2X-VC integration. (b) Seasonal variation of the difference in surface water budget of the Great Plains region between the 2X-VC and 1X-VC integrations. (Solid line: Δr; dashed line: $-\Delta e$; Dotted line: $-\Delta f$; dash-dotted line: Δm; and large dot: $\partial \Delta W/\partial t$.) Units are cm day^{-1}. (c) Seasonal variation of the difference in surface heat budget of the Great Plains region between the 2X-VC and 1X-VC integrations. (Solid line: ΔDSR; dotted line: −ΔULR; dash-dot-dot-dotted line: −ΔSH; dashed line: −ΔLH; dash-dotted line: −ΔLM.) Units are in W m^{-2}.

The positive feedback process for soil moisture reduction described before is indicated in Fig. 17c which illustrates, for the Great Plains region, the annual marches of the difference in various components of surface heat balance between the 2X-VC and 1X-VC integrations. This figure shows a large surface heat gain during the summer months due to the marked increase in the absorption of solar energy. The increased absorption results from the reduction of total cloud amount previously described. It is much larger than the surface heat loss resulting from the decrease of downward long wave radiation due to the reduced cloud cover. The figure also indicates that, in summer, the Great Plains surface gains heat due to the reduction of evaporation and loses heat because of the increase in sensible heat flux. Both of these changes result from a large reduction of soil moisture in summer. The features of the CO_2-induced changes in heat budget of the Great Plains region of the VC model described previously are quite different from those of the FC model revealing the profound effect of the cloud-land surface interaction upon the hydrology of the Great Plains.

In summary, soil wetness over the Great Plains of both FC and VC models decreases in response to an increase of atmospheric carbon dioxide. In qualitative agreement with the behavior of the FC model, this reduction results from the earlier commencement of the spring to summer reduction of soil moisture due to the earlier terminations of the snowmelt season and the rainy period in spring. In the VC model, the dryness is enhanced further by a positive feedback process involving the change of cloud cover.

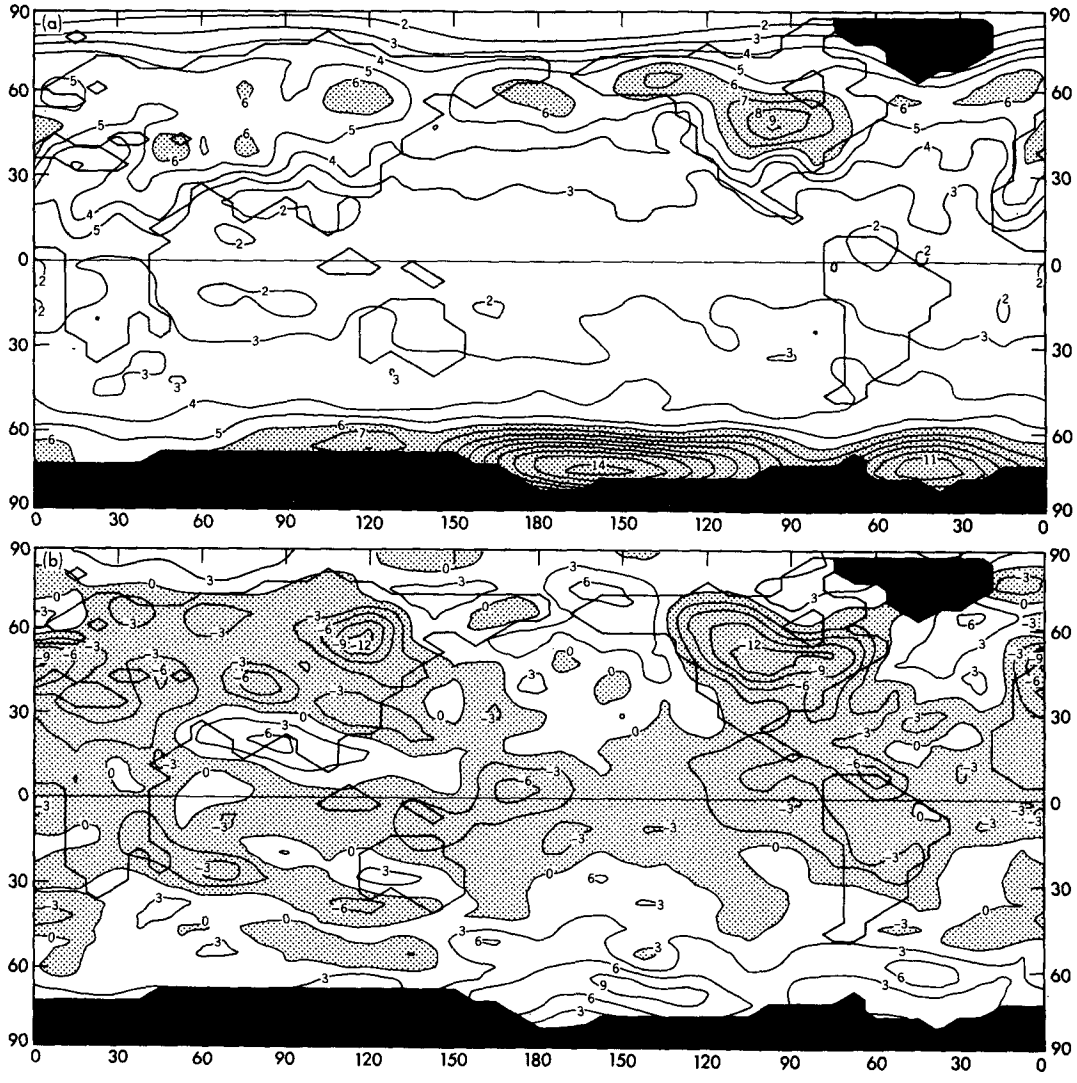

FIG. 18. (a) Geographical distribution of the difference in surface air temperature (averaged over the 3-month period of June, July and August) between the 2X-VC and 1X-VC integrations. Units are in °C. (b) Geographical distribution of the difference in total cloud amount (%) between the 2X-VC and 1X-VC integrations.

c. *Southern Europe*

The FC Model. The seasonal variations of soil moisture obtained from the 4X-FC and 1X-FC integrations are illustrated in Fig. 10c. In both cases, soil moisture approaches saturation in winter but rapidly reduces and becomes very small in summer. Compared with the Great Plains, it begins to decrease earlier and reaches a substantially lower level during summer. In the 4X-FC case, the summer value of soil moisture is only 60% of the corresponding value in the 1X-FC case indicating that it is reduced substantially in response to the quadrupling of atmospheric CO_2.

The seasonal variation of the surface water budget is analyzed for both the 4X-FC and 1X-FC experiments and is illustrated in Fig. 19a, b. In addition, the annual marches of the difference in various components of water budget between the two experiments are shown in Fig. 19c in order to evaluate the influence of CO_2-quadrupling upon the surface water budget of the FC model.

In general, the annual variations of the components of surface water budget over southern Europe resemble those over the Great Plains. For example, the difference in rainfall between the two integrations is rapidly reduced from March to June and becomes negative in summer contributing to the CO_2-induced summer reduction of soil moisture. However, both snowfall and snowmelt over western Europe are smaller than that over the Great Plains in spring and have a relatively small contribution to the surface water budget of the warm season.

The VC-Model. The seasonal variations of the difference in water budget between the 2X-VC and 1X-VC models are similar to the results from the FC model that has been described. The difference in the contribution from rainfall, however, is more negative during summer particularly in June and July producing an extreme drought. This is due to the positive feedback process involving cloud and land surface as discussed in the preceding subsection on the Great Plains. In summary, the CO_2-induced change in the water budget of southern Europe shown here is qualitatively similar to the corresponding change over the Great Plains except that the influence of spring snowmelt is smaller.

d. *Northern Siberia*

Over the zonal belt along the northern edge of the Eurasian continent, the seasonal variations of soil moisture and their CO_2-induced changes in both FC- and VC models are qualitatively similar to the variations over the North Canadian region. (Compare, for example, Fig. 10a, which illustrates the soil moisture variations over northern Canada and Northern Siberia of the FC-model.) Therefore, the detailed analysis of the seasonal water budget over the northern Siberian region is not shown here.

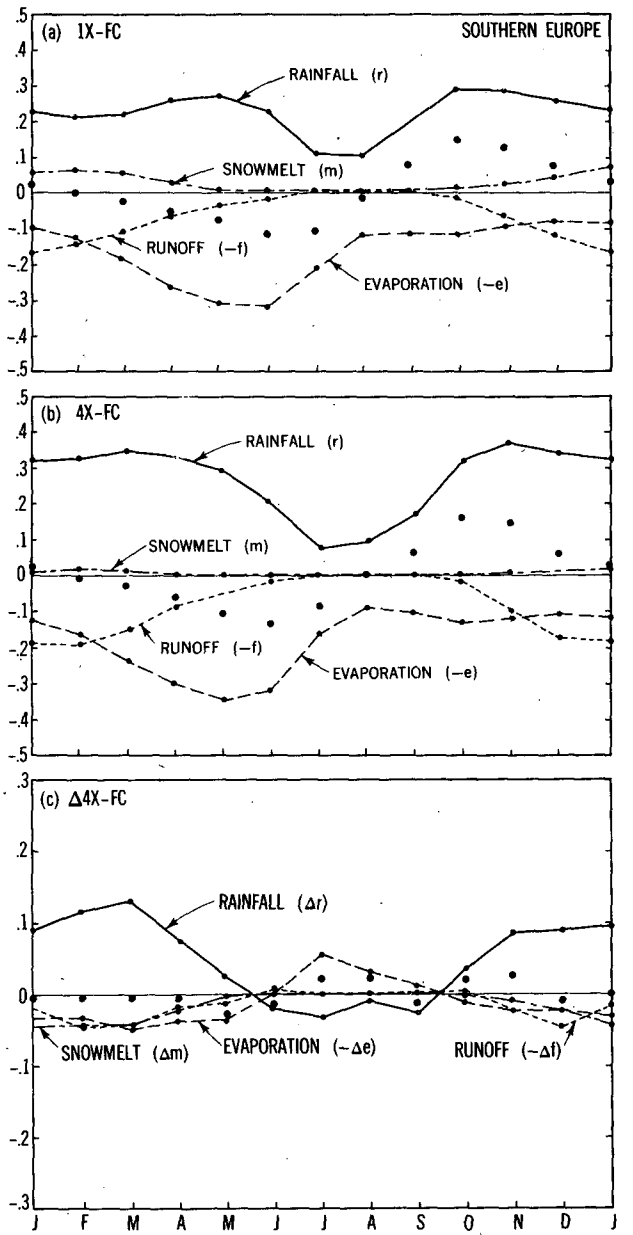

FIG. 19. Seasonal variation of the surface water budget averaged over the southern Europe region of the FC model. (a) 1X-FC integration, (b) 4X-FC integration and (c) 4X- minus 1X-FC integrations. (Solid line: r or Δr; dashed line: $-e$ or $-\Delta e$; dotted line: $-f$ or $-\Delta f$; dash-dotted line: m or Δm; large dot: $\partial W/\partial t$ or $\partial \Delta W/\partial t$.) Units are in cm day^{-1}.

6. Conclusion

Based upon the results from global climate models developed at the Geophysical Fluid Dynamics Laboratory, it is suggested that soil wetness decreases in summer over extensive midcontinental regions in middle and high latitudes in response to an increase of atmospheric carbon dioxide. These regions of reduced soil moisture include the Great Plains of North

America, southern Europe, northern Canada and northern Siberia.

It is shown that the CO_2-induced reduction of soil moisture in summer over the northern parts of Siberia and Canada in this model is due to the earlier termination of the snowmelt season followed by a period of enhanced evaporation. The earlier commencement of the period of enhanced evaporation initiates a dryer soil condition which persists throughout summer in high latitudes.

Over the Great Plains of North America, the earlier termination of the snowmelt season followed by the period of enhanced evaporation also contributes to the CO_2-induced reduction of soil moisture in summer. In addition, the change in precipitation rate in middle latitudes contributes to the summer reduction. As indicated in the results from previous studies (see, for example, Manabe, 1983), the CO_2-induced warming of the present model increases with increasing latitudes. Therefore, the warm, moisture-rich air in a high CO_2-atmosphere can penetrate into higher latitudes than it can for the normal CO_2-atmosphere. Thus, the rate of precipitation increases markedly in the northern part of the middle latitude rainbelt, whereas it reduces in the southern part. Because the rainbelt shifts polewards from winter to summer, a region in the middle latitudes, which is located in the northern part of the rainbelt in winter, would be in the southern part in summer. Therefore, the CO_2-induced change in precipitation rate is reduced rapidly from a large positive to a negative value as the season progresses from spring to summer contributing to the reduction of soil moisture during this period.

In the model with variable cloud cover, the CO_2-induced reduction of soil moisture over the Great Plains in summer is further enhanced due to the positive feedback process involving a change in cloud cover. When soil moisture is reduced, a larger fraction of radiative energy absorbed by the continental surface is ventilated through the upward flux of sensible heat rather than evaporation. Accordingly, the temperatures of the continental surface and the overlying layer increase resulting in the general reduction of relative humidity and precipitation in the lower model troposphere. Accompanying the reduction of relative humidity, total cloud amount also reduces causing an increase of solar energy reaching the continental surface. Thus, the radiative energy absorbed by the continental surface also increases. Both the decrease of precipitation and the increase of absorbed radiative energy mentioned above further reduce soil moisture during early summer and help to maintain it at a low level throughout the summer.

Over southern Europe, the CO_2-induced reduction of soil moisture in summer occurs in a qualitatively similar manner. However, the contribution of snowmelt is much smaller than its contribution over the Great Plains described in the preceding paragraph.

The numerical experiments conducted in the present study indicate that the CO_2-induced changes of soil wetness in middle and high latitudes reverse sign as the season progresses from summer to winter. In the results from both the FC- and VC-models, soil wetness over the Eurasian and North American continents increases in winter polewards of 30°N in response to an increase in atmospheric carbon dioxide. Over northern Canada and Northern Siberia where the warming of the near surface layer of the model atmosphere is pronounced, precipitation increases markedly in winter due to the penetration of warm, moisture-rich air into high latitudes. Because of the warming, a larger fraction of this increased precipitation is realized as rainfall, and snowmelt is enhanced maintaining the soil moisture at a high level until the late spring.

Over the Great Plains of North America and other midcontinental regions of the Northern Hemisphere in middle latitudes, soil wetness is also enhanced during winter in response to an increase of atmospheric carbon dioxide. Since the middle-latitude rainbelt is located at a lower latitude in winter, these regions are situated under the northern half of the rainbelt where the CO_2-induced change of precipitation rate is positive due to the increased poleward moisture transport. In a warm, CO_2-rich environment, a larger fraction of the increased precipitation is realized as rainfall enhancing further the wetness of the soil during winter.

In this investigation, the CO_2-induced changes in soil wetness are determined from the equilibrium response of these models to an increase in atmospheric carbon dioxide. Accordingly, the hydrologic response obtained here may be different from the transient response of climate to a gradual increase in atmospheric carbon dioxide. However, the results from the present analysis suggest that the midcontinental soil moisture is reduced in summer through a relatively simple process dictated by the surface warming which increases with increasing latitudes. Therefore, it is likely that the very broad-scale features of the summer reduction of soil wetness described in this study will also emerge in the transient response of climate to an increase of atmospheric carbon dioxide. To confirm this speculation, it is necessary to investigate the transient response of climate by use of a model with more realistic oceans. This is a subject for future investigation.

Acknowledgment. The authors are very grateful to A. J. Broccoli and R. J. Stouffer for assisting with the construction of the versions of the atmosphere-mixed layer ocean model used for the present study. A. J. Broccoli, T. Delworth, and H. Levy II read the first draft of the paper and made many valuable suggestions for improving it. J. Kennedy, P. Tunison and J. Conner assisted in the preparation of the manuscript.

APPENDIX

Poleward Transport of Water Vapor

In section 5 it was noted that the reduction of precipitation rate in the southern part of the middle-lati-

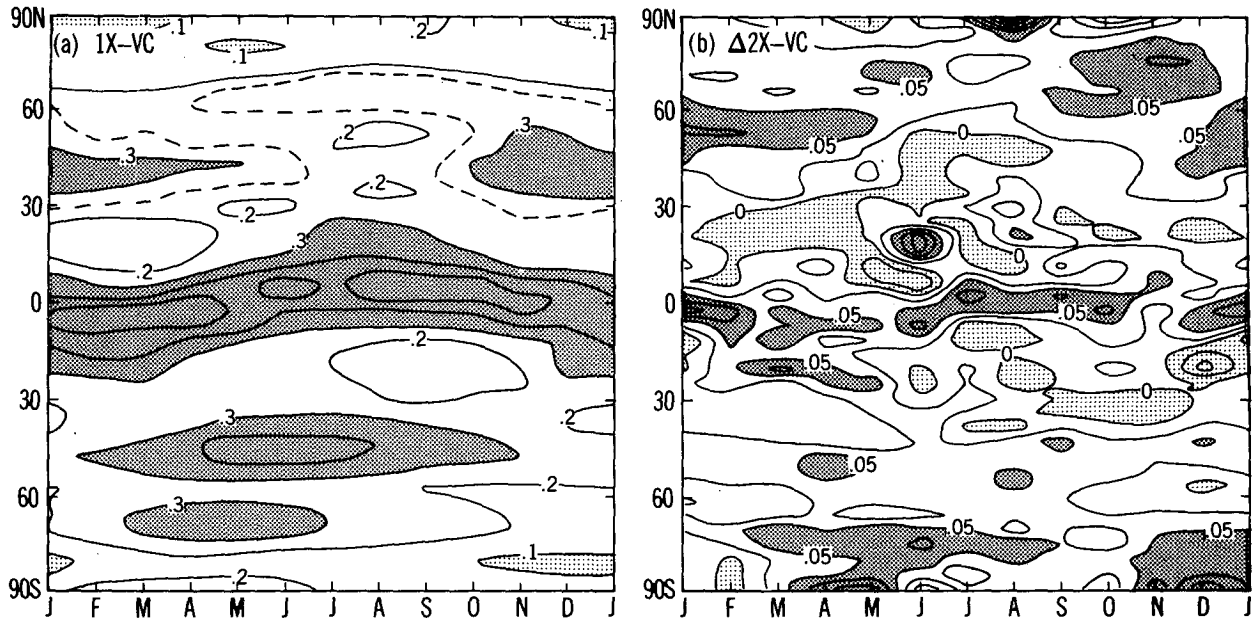

FIG. A1. (a) The latitude–month distribution of the zonally averaged, monthly mean rate of precipitation (cm day^{-1}) from the 1X-VC integration. (b) The latitude–month distribution of the difference in zonally averaged, monthly mean rate of precipitation (cm day^{-1}) between the 2X- and 1X-VC integrations.

tude rainbelt is partly responsible for the CO_2-induced summer drought over the Great Plains of North America and western Europe. Qualitatively similar changes in precipitation rate also occur in other midcontinental regions of the middle latitudes. This is evident in Fig. A1 which illustrates the seasonal and latitudinal distribution of zonal mean precipitation rate and its CO_2-induced change obtained from the VC model. (Here, the zonal averaging is made over an entire latitude circle.) As this figure illustrates, the middle latitude rainbelt shifts polewards as the seasons proceed from winter to summer and returns to the original position in the

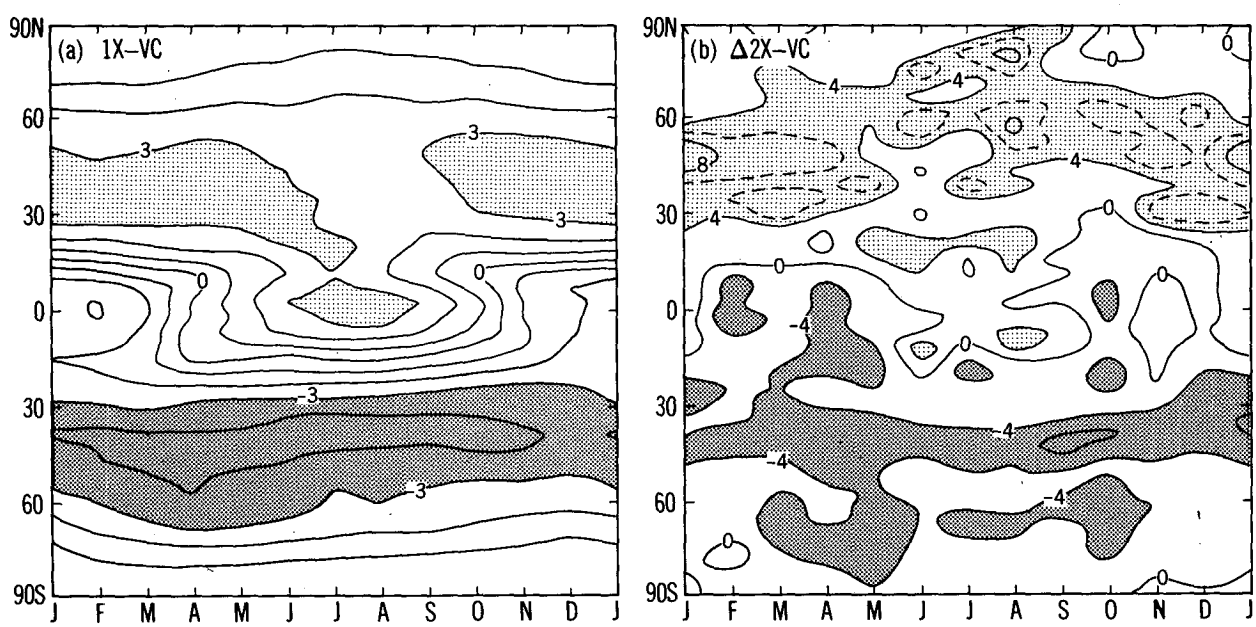

FIG. A2. (a) The latitude–month distribution of the northward atmospheric moisture transport from the 1X-VC integration. Units are in g m sec^{-1}. (b) The latitude–month distribution of the difference in northward atmospheric moisture transport between the 2X- and 1X-VC integrations. Units are in 10^{-1} g m sec^{-1}.

fall. In response to the doubling of the atmospheric carbon dioxide, the rate of precipitation increases over the northern part of the rainbelt, whereas it is reduced in the southern half. To evaluate how such changes in precipitation rate occur, the poleward moisture transport and its CO_2-induced change are analyzed and are the subject of discussion in this Appendix.

Fig. A2b illustrates the latitude-month distribution of the difference in zonally averaged northward moisture transport between the 2X- and the 1X-VC integrations. For reference, the latitude–month distribution of atmospheric moisture transport from the 1X-VC case is also shown in Fig. A2a. In this figure, the northward moisture transport in the model atmosphere is defined by

$$\frac{1}{g}\int_0^{p_*} \overline{vr}^{\lambda} dp$$

where g is the acceleration of gravity, p pressure, p_* surface pressure, v the northward component of wind, r the mixing ratio of water vapor in air and $(\bar{\ })^{\lambda}$ denotes the zonal average over an entire latitude circle.

According to Fig. A2b, the northward moisture transport in the northern Hemisphere of the VC-model increases significantly at about 45°N in winter and at about 60°N in summer in response to the doubling of atmospheric carbon dioxide. The reason why the poleward moisture transport in the Northern Hemisphere of the VC-model changes as described before has not been identified in a rigorous manner. It appears, however, that one of the important factors which affects the change in moisture transport is the CO_2-induced rise of the temperature of the lower troposphere which increases with increasing latitude. Such warming raises the water vapor content of air enhancing the poleward moisture transport by the model atmosphere particularly in high latitudes.

The CO_2-induced change in moisture transport previously described enhances the removal of water vapor from the southern part of the middle latitude rainbelt and adds moisture to the northern part. Thus, the rate of precipitation is reduced in the southern part and increases in the northern part of the rainbelt. Such change is evident in Fig. A1b.

The result described here indicates that the change in moisture transport due to the CO_2-induced warming alters the distribution of precipitation contributing to the summer reduction of soil wetness as discussed in section 5.

REFERENCES

Berlyand, T. G., L. A. Strokina and L. E. Greshnikova, 1980: Zonal cloud distribution on the earth. *Meteor. Gidrol.*, **3**, 15–23.

Bryan, K., 1969: Climate and ocean circulation. II: The ocean model. *Mon. Wea. Rev.*, **97**, 828–829.

Gordon, C. T., and W. F. Stern, 1982: A description of the GFDL global spectral model. *Mon. Wea. Rev.*, **110**, 625–644.

Hansen, J., A. Lacis, D. Rind, G. Russel, P. Stone, I. Fung, R. Ruedy and J. Lerner, 1984: Climate Sensitivity: Analysis of Feedback Mechanisms. 130–163 in *Climate Process and Climate Sensitivity* (Maurice Ewing Series, 5) edited by J. E. Hansen and T. Takahashi, American Geophysical Union, Wash., D.C.

London, J., 1957: A study of atmospheric heat balance. Final Report. Contract AF19(122)-165 DDC College of Engineering, New York University. [NTIS AD 117227].

Lvovitch, M. I., and S. P. Ovtchinnikov, 1964: Physical-geographical atlas of the world (in Russian). Acad. of Sciences, U.S.S.R., and Department of Geodesy and Cartography, State Geodetic Committee, Moscow (see p. 61).

Manabe, S., 1969: Climate and ocean circulation. I. The atmospheric circulation and the hydrology of the earth's surface. *Mon. Wea. Rev.*, **97**, 739–774.

——, 1983: Carbon dioxide and climatic change. In "Theory of Climate." *Adv. Geophys.*, **20**, 39–82.

——, and R. J. Stouffer, 1980: Sensitivity of a global climate model to an increase of CO_2-concentration in the atmosphere. *J. Geophys. Res.*, **85**, 5529–5554.

——, and A. J. Broccoli, 1985: A comparison of climate model sensitivity with data from the last glacial maximum. *J. Atmos. Sci.*, **42**, 2643–2650.

——, and R. T. Wetherald, 1985: CO_2 and hydrology in "Issues in Atmospheric and Oceanic Modeling." *Adv. in Geophys.*, **28**, Part A, 131–157.

——, and ——, 1986: Reduction in summer soil wetness induced by an increase in atmospheric carbon dioxide. *Science*, **232**, 626–628.

——, —— and R. J. Stouffer, 1981: Summer dryness due to an increase of atmospheric CO_2 concentration. *Climatic Change*, **3**, 347–386.

——, J. Smagorinsky and R. F. Strickler, 1965: Simulated climatology of a general circulation model with a hydrologic cycle. *Mon. Wea. Rev.*, **93**, 769–778.

Mitchell, J. F. B., and G. Lupton, 1984: A $4 \times CO_2$ integration with prescribed changes in sea surface temperatures. *Progress in Biometeorology*, **3**, 353–374.

National Academy of Sciences, U.S., 1983: Changing Climate. National Academy Press, Washington, DC.

Posey, J. W., and P. F. Clapp, 1964: Global distributions of normal surface albedo. *Geofis. Int.*, **4**, 33–84.

Schlesinger, M. E., and J. F. B. Mitchell, 1985: Model projection of the equilibrium climatic response to increasing carbon dioxide, 81–148, in *Potential Climatic Effects of Increasing Carbon Dioxide* DOE/ER-0237. Edited by M. C. McCracken and F. M. Luther, U.S. Dept. of Energy.

Vinnikov, K. Ya., and P. Ya. Groisman, 1982: The empirical study of climate sensitivity. Izvestiya, atmospheric and oceanic physics, Academy of Science, U.S.S.R. **18**(11), 1159–1169.

Washington, W. M., and G. A. Meehl, 1984: Seasonal cycle experiments on the climate sensitivity due to a doubling of CO_2 with an atmospheric general circulation model coupled to a simple mixed layer ocean model. *J. Geophys. Res.*, **89**(D6), 9475–9503.